



Cite this: *Lab Chip*, 2024, **24**, 1833

## Recent developments and future perspectives of microfluidics and smart technologies in wearable devices

Sasikala Apoorva,<sup>a</sup> Nam-Trung Nguyen  <sup>b</sup> and Kamalalayam Rajan Sreejith\*<sup>b</sup>

Wearable devices are gaining popularity in the fields of health monitoring, diagnosis, and drug delivery. Recent advances in wearable technology have enabled real-time analysis of biofluids such as sweat, interstitial fluid, tears, saliva, wound fluid, and urine. The integration of microfluidics and emerging smart technologies, such as artificial intelligence (AI), machine learning (ML), and Internet of Things (IoT), into wearable devices offers great potential for accurate and non-invasive monitoring and diagnosis. This paper provides an overview of current trends and developments in microfluidics and smart technologies in wearable devices for analyzing body fluids. The paper discusses common microfluidic technologies in wearable devices and the challenges associated with analyzing each type of biofluid. The paper emphasizes the importance of combining smart technologies with microfluidics in wearable devices, and how they can aid diagnosis and therapy. Finally, the paper covers recent applications, trends, and future developments in the context of intelligent microfluidic wearable devices.

Received 29th January 2024,  
Accepted 23rd February 2024

DOI: 10.1039/d4lc00089g

rsc.li/loc

### 1. Introduction

Wearable devices have transformed healthcare and personal wellness by providing affordable and convenient options for continuous patient monitoring.<sup>1</sup> In contrast to traditional clinical diagnostics, wearable devices can provide real-time data on an individual's health using non-invasive or minimally invasive methods, making them an attractive option for healthcare monitoring.<sup>2</sup> For instance, wearable devices such as Fitbit,<sup>3</sup> Apple Watch,<sup>4</sup> and Garmin<sup>5</sup> are commonly used for tracking fitness metrics, while other devices such as continuous glucose monitors<sup>6</sup> and ECG monitors<sup>7</sup> are used for medical purposes such as monitoring blood sugar levels and heart activity. Although these devices initially struggled to gain acceptance, the COVID-19 pandemic has accelerated their adoption in healthcare.<sup>8</sup> According to the forecast of Gartner Inc., the global end-user expenditure on wearable devices was forecasted to reach \$93.8 billion in 2022, with most customers relying on smartwatches for fitness monitoring and smart patches for health monitoring (Fig. 1).<sup>9</sup>

To address the need for more specific data collection from wearable devices, microfluidics has been incorporated into

wearable sensors, allowing medical experts to continuously acquire specific high-quality data from patients.<sup>10,11</sup> By combining microfluidic wearable sensors with other wearable technologies, such as gyroscopes, accelerometers, and temperature sensors, real-time bodily fluids can be analysed with continuous tracking.<sup>12</sup> These integrated devices offer high throughput, high sensitivity, and low power consumption.<sup>13</sup> Wearable sensors that attach to the skin

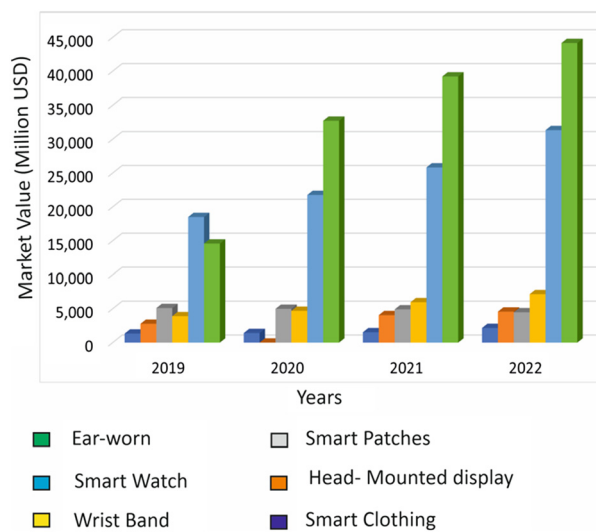


Fig. 1 The market value of wearable devices for health monitoring worldwide.

<sup>a</sup> UKF Centre for Advanced Research and Skill Development(UCARS), UKF College of Engineering and Technology, Kollam, Kerala, India, 691 302

<sup>b</sup> Queensland Micro and Nanotechnology Centre, Griffith University, 170 Kessels Road, Nathan, 4111, Queensland, Australia.

E-mail: s.kamalalayamrajan@griffith.edu.au

surface can measure temperature, heart rate, blood sugar, and other vitals more accurately than other wearables, making them an attractive option for monitoring health.<sup>14</sup> Microfluidics can also be used for on-site therapy and precise delivery of drugs or pharmaceuticals.<sup>15,16</sup>

Incorporating smart intelligent technologies such as artificial intelligence (AI), machine learning (ML), and Internet of Things (IoT) into wearable devices has several technical advantages. AI algorithms can analyse vast amounts of data collected by wearable sensors, allowing for a more accurate and detailed assessment of an individual's health status.<sup>17</sup> This analysis takes into account not only an individual's vital signs, but also other relevant factors such as age, sex, and geographic region. By determining the normal range of vital signs for specific populations, healthcare professionals can provide more personalized recommendations for treatment and monitoring.<sup>18</sup> This personalized approach leads to the development of individualized health profiles that provide better accuracy in diagnosing and treating diseases.<sup>19</sup> The integration of AI with Internet of Things (IoT) platforms further enhances the capabilities of wearable devices, allowing for real-time monitoring and communication with healthcare professionals.<sup>20,21</sup> The incorporation of these intelligent technologies in wearable devices can ultimately lead to the development of a more personalized approach to healthcare, with the ability to predict and prevent disease, improving overall wellness.<sup>17</sup>

These exciting developments make clear that the future of healthcare is strongly linked to the integration of smart technologies and microfluidics in wearable devices. The potential benefits of such integration are numerous.<sup>22</sup> However, there are challenges to be addressed, including the development of algorithms that can accurately interpret and make sense of the vast amount of data generated by microfluidic wearable sensors, and ensuring that the technology is accessible and affordable to all patients.<sup>23</sup>

To fully realize the potential of smart microfluidic wearable devices in healthcare, it is crucial to continue investing in research and development, as well as promoting collaboration between experts in the fields of AI, microfluidics, and healthcare. Considering this objective, the present review focuses on non-invasive and minimally invasive microfluidic wearable sensors, for analysis, diagnosis and monitoring. The novelty of this review is that it emphasises the combination of emerging smart technologies and microfluidics, and how it can aid diagnosis and therapy of wearable devices. Furthermore, recent applications, recent trends, and future developments in smart microfluidic wearable devices are also provided.

## 2. Microfluidics in wearable devices

Microfluidics is a rapidly growing research field that focuses on the manipulation of fluids on the microscale, with typical dimensions of microchannels less than 1 mm.<sup>11,15,24</sup> This field has been the subject of numerous theoretical studies

aiming at more efficient processes and devices for applications in chemistry, biology, and medicine.<sup>25,26</sup> Microfluidic technologies are well-suited for a variety of applications due to their advantages of low volumes, high sensitivity, rapid processing, high spatial resolution, and high integration with sensing components.<sup>15,27,28</sup> The ease and low cost of fabrication, prototyping, and implementation have also played an important role in the success of microfluidic technology.

In the field of wearable devices, microfluidics has seen significant growth, particularly for healthcare applications. By controlling and manipulating small amounts of bodily fluids on the microscale, microfluidics enables more accurate and precise analysis of these fluids, essential for continuously monitoring a patient's health.<sup>29</sup> Small changes in bodily fluids can provide critical information about a patient's health status, making microfluidics a valuable tool in healthcare monitoring.<sup>30</sup> As mentioned earlier, microfluidics can also be used for the precise delivery of drugs or other therapeutic agents, enhancing the effectiveness of treatment.

The miniaturization of microfluidic components makes integrating this technology into wearable devices possible, allowing for portability and ease of use.<sup>31</sup> Microfluidic technology is offering a promising solution for non-invasive and real-time monitoring.<sup>13</sup> Wearable devices that incorporate microfluidic channels can provide valuable information about a wearer's health status, including electrolyte levels and biomarkers, which enables the diagnosis and management of a range of health conditions.<sup>32</sup>

The potential applications of microfluidic wearable devices are not limited to healthcare alone. This technology has the potential to be utilized in environmental monitoring, food safety, and sports performance.<sup>33,34</sup> For instance, microfluidic wearable devices can be used to monitor environmental pollutants or detect contaminants in food products. In sports, these devices can be used to monitor the electrolyte levels of athletes during training and competition.<sup>35</sup>

The proper functioning of a microfluidic device depends on careful consideration of each step of the development process, from design to fabrication, to analysis and to signal processing.<sup>36</sup> The fabrication of a microfluidic device involves designing and manufacturing microchannels, chambers, and valves using materials such as glass, silicon, or polymers.<sup>25,37,38</sup> Appropriate sample collection and storage methods are crucial to ensure accurate and reliable results. Various techniques can be employed depending on the type of sample being analysed. Sample analysis is the core component of a microfluidic device and involves a range of methods such as optical, electrochemical, and biological assays, to detect and quantify analytes such as biomarkers.<sup>39</sup> Within microfluidic wearable devices, signal transduction and amplification processes play a crucial role in transforming subtle signals from samples into easily interpretable data. Concurrently, mechanical sensing mechanisms ensure the precise handling and delivery of these minuscule samples, significantly enhancing the accuracy of measurements and analyses. Finally, the device must be

powered, which can be achieved through various means, such as batteries or external power sources.<sup>40,41</sup>

Polydimethylsiloxane (PDMS),<sup>42</sup> paper microfluidics,<sup>25</sup> and patches with microneedles<sup>43</sup> are microfluidic technologies that have unique features and advantages for various applications. The following sections provide a detailed discussion on the applications of the aforementioned technologies and their corresponding features.

## 2.1. PDMS-based microfluidics

Microfluidic devices for manipulating small volumes of fluids are commonly made from polymers due to their biocompatibility, flexibility, and cost-effectiveness.<sup>44</sup> Techniques for manufacturing polymer-based microfluidic devices include soft lithography,<sup>45</sup> hot embossing,<sup>46</sup> and injection moulding,<sup>47</sup> with soft lithography being the most widely used.<sup>48</sup> Polydimethylsiloxane (PDMS) is the most commonly used polymer for fabricating microfluidic devices.<sup>49</sup> Other than PDMS, other polymers are polystyrene (PS),<sup>50</sup> polyether ether ketone (PEEK),<sup>51</sup> polyethylene terephthalate (PET),<sup>52</sup> polyvinyl chloride (PVC),<sup>53</sup> polymethylmethacrylate (PMMA),<sup>54</sup> cyclic olefin copolymer (COC),<sup>55</sup> polycarbonate (PC),<sup>56</sup> and polyetherimide (PEI)<sup>57</sup> that are used for making microfluidic devices.<sup>58</sup>

PDMS belongs to the siloxane family and is a type of mineral organic polymer. PDMS is highly suitable for lab-on-a-chip (LOC) applications,<sup>59</sup> and its unique properties make it a primary choice for researchers and developers working on microfluidic devices and wearable sensors. PDMS has a low Young's modulus, allowing it to easily conform to and wrap around curved surfaces.<sup>60</sup> This property also makes it a popular choice for providing conformal contact with different surfaces. Its elasticity and flexibility are highly desirable properties of wearable devices.<sup>61</sup> PDMS is relatively low-cost compared to other materials used for microfluidics. The transparency of PDMS allows for easy visualization of the fluid content and all other components.<sup>62</sup> These features make PDMS ideal for serving as a foundational material for wearable electronic devices like fitness trackers. Researchers commonly use two types of PDMS, PDMS RTV-615 and PDMS Sylgard 184, for microfluidic applications.<sup>63</sup> However, the exact composition of these two PDMS types is not disclosed by the vendors.

Researchers have developed innovative ways to utilize PDMS in wearable microdevices. For example, Trinh *et al.* developed a wearable microdevice that uses flexible and soft-contact PDMS for the amplification of nucleic acids through recombinase polymerase amplification (RPA).<sup>38</sup> The PDMS was mixed with different ratios of the pre-polymer and a curing agent without altering the fundamental properties of PDMS. The team demonstrated that the basic characteristics of PDMS remained consistent despite the change in the prepolymer and curing agent ratio. The replica moulding technique was used to build the wearable PDMS microdevice with microchambers for RPA reagents. It required soft

lithography to create a mould on a PET film, pouring and curing pre-polymer PDMS, and then adhering it to a thin PDMS film. For RPA tests, the flexible device adhered to human skin. The wearable RPA microdevice contained procedures for loading RPA reagents and carrying out reactions both before and after it was attached to a person's skin. To prevent sample loss during movement, a thin PDMS sheet was placed over the microdevice chamber during reactions. The microdevice was taken out after the reaction to be used for RPA result analysis. Fig. 2a shows the typical operation of the wearable PDMS device.

On the other hand, Heo *et al.* developed a collagen–PDMS composite material that maintains the soft elastomer properties needed for skin-interfaced microfluidics while reducing water evaporation.<sup>64</sup> The skin-interfaced collagen–PDMS microfluidic device enhances sweat retention by 45% over a period of 9 hours compared to pure PDMS. Fig. 2b shows an exploded view of the device with layers including a cover layer, an indicator dye, a channel layer and adhesive.

While PDMS is widely used in the fabrication of microfluidic devices, the material has limitations. For instance, PDMS may age over time, limiting the intended performance. Additionally, PDMS is not highly compatible with many organic solvents, absorbing hydrophobic molecules and water vapour, which can be inadvertently emitted during experiments.<sup>65</sup> One major drawback of PDMS microfluidic devices is the inability to integrate electrodes within the device.<sup>66</sup> However, this can be overcome by placing electrodes on a glass cover slide instead of directly on the chip.

## 2.2. Paper-based microfluidics

Existing diagnostic technologies are often expensive and inaccessible. This bottleneck can be addressed by paper-based microfluidic devices.<sup>67</sup> As an inexpensive and lightweight substrate, paper is an ideal option for microfluidic devices that are portable for immediate use.<sup>68</sup> These devices are made by patterning paper with hydrophobic structures to define hydrophilic channels that transport fluid through capillary action.<sup>69</sup> While most devices use colorimetric assays,<sup>70</sup> electrochemical,<sup>71</sup> chemiluminescence,<sup>72</sup> and electrochemiluminescence<sup>71</sup> methods can also be employed in paper-based devices. Techniques such as wax printing,<sup>73</sup> inkjet printing,<sup>74</sup> photolithography,<sup>75</sup> flexographic printing,<sup>76</sup> plasma treatment,<sup>77</sup> laser treatment,<sup>78</sup> wet etching,<sup>79</sup> and screen printing<sup>80</sup> have been utilised for fabricating paper-based microfluidic devices. Among these, wax printing is the simplest method.

Mogera *et al.* introduced a wearable microfluidic system with plasmonic sensors on paper for continuous monitoring of sweat loss, sweat rate, and its constituent metabolites.<sup>81</sup> This soft, flexible, and stretchable system covers the skin without causing any physical or chemical irritations. Fig. 2c shows the conceptual diagram of the device. Similarly,

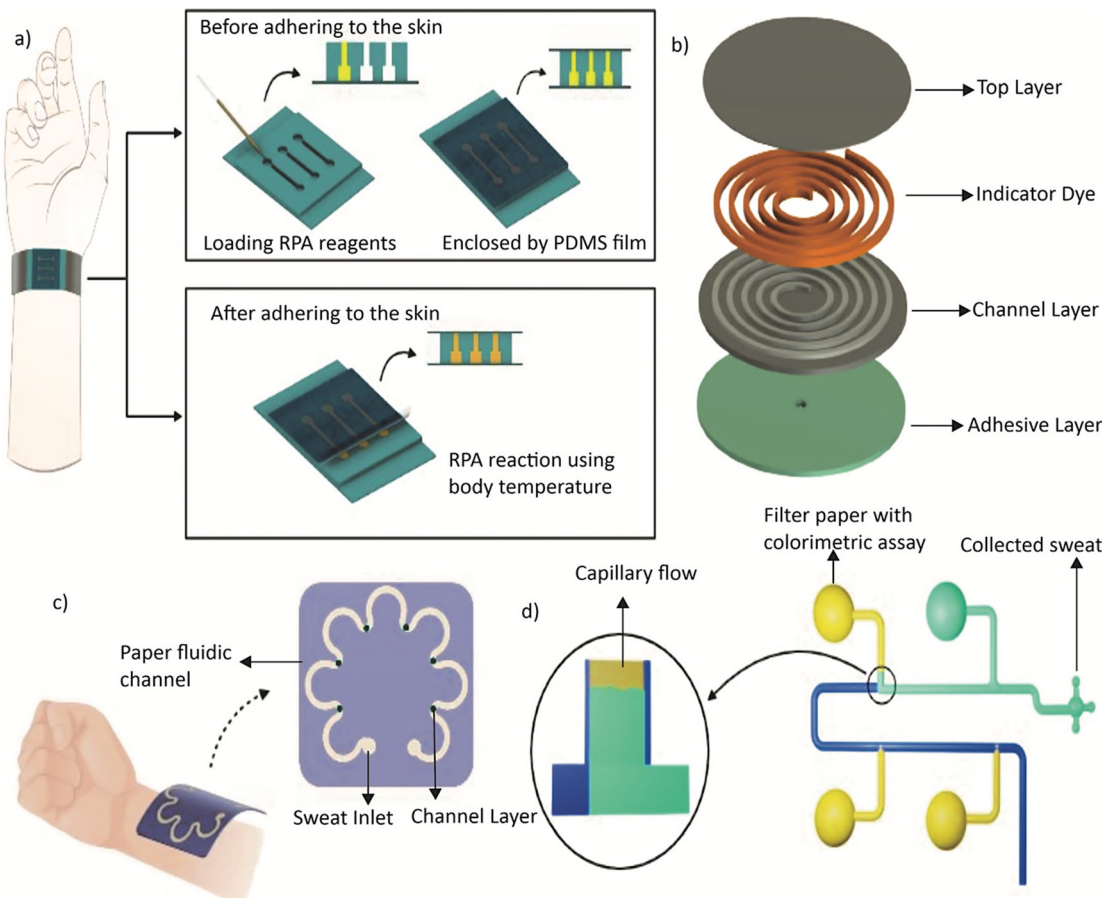


**Fig. 2** a) Schematic illustration showing the operation of a wearable microdevice that uses flexible and soft-contact PDMS for the amplification of nucleic acids through RPA. b) Exploded view of the sweat collection device by Heo *et al.*, including a cover layer, an indicator dye, a channel layer, and adhesive. c) Conceptual diagram of a wearable plasmonic paper-based microfluidic device by Mogera *et al.* d) Schematic illustration of a paper-integrated microfluidic device for sequential analysis of sweat that eliminates the need for air exits in a reservoir.

Abbasiasl *et al.* presented an easy-to-fabricate paper-integrated microfluidic device for sequential analysis of sweat that eliminates the need for air exits in each reservoir, thereby reducing the negative effects of sweat evaporation.<sup>82</sup> Fig. 2d illustrates the top and bottom views of this device. By directing liquid sequentially into the chambers using the high capillary force of filter paper, the device enables further chemical analysis. Researchers employed colorimetric assays to demonstrate the device's performance in chrono-analysis of glucose standard solutions and pH of sweat during exercise. The findings indicate the potential of this approach to sequentially analyse the concentration of biomarkers over a specific period.

Paper-based microfluidic devices have several advantages over traditional substrates such as glass and PDMS, including low cost, disposability, and portability.<sup>83</sup> However, liquid transport with patterned channels can be challenging on paper compared to other substrates due to the fibrous and porous nature of paper.<sup>84</sup> Despite this issue, the affordability and simplicity of paper-based microfluidic devices make them an attractive option for developing wearable devices and other portable diagnostic tools.

### 2.3. Microneedle-based transdermal microfluidics

Microneedle-based transdermal microfluidics is a revolutionary technology that combines microneedles and microfluidics to deliver drugs and therapeutics transdermally.<sup>85</sup> Microneedles, typically smaller than a millimetre, create tiny channels in the skin that allow for transdermal drug delivery, while microfluidics involves microchannels embedded in a patch to transport and deliver chemicals to the microneedles.<sup>86</sup> The integration of microneedles with microfluidics offers several potential advantages over traditional drug delivery methods, such as increased efficiency, reduced side effects, and improved patient compliance.<sup>87</sup>

There are four types of microneedles: solid, coated, polymeric (dissolvable), and hollow microneedles. Fig. 3a shows the schematic diagram of the different types of microneedles.<sup>88</sup> Solid microneedles puncture the skin to create channels for drug delivery and cause less pain than traditional needles.<sup>89</sup> Microneedles can be made from various materials such as silicon, metals, polymers, or ceramics. Following the insertion, a drug formulation can be applied to the skin using a patch or a

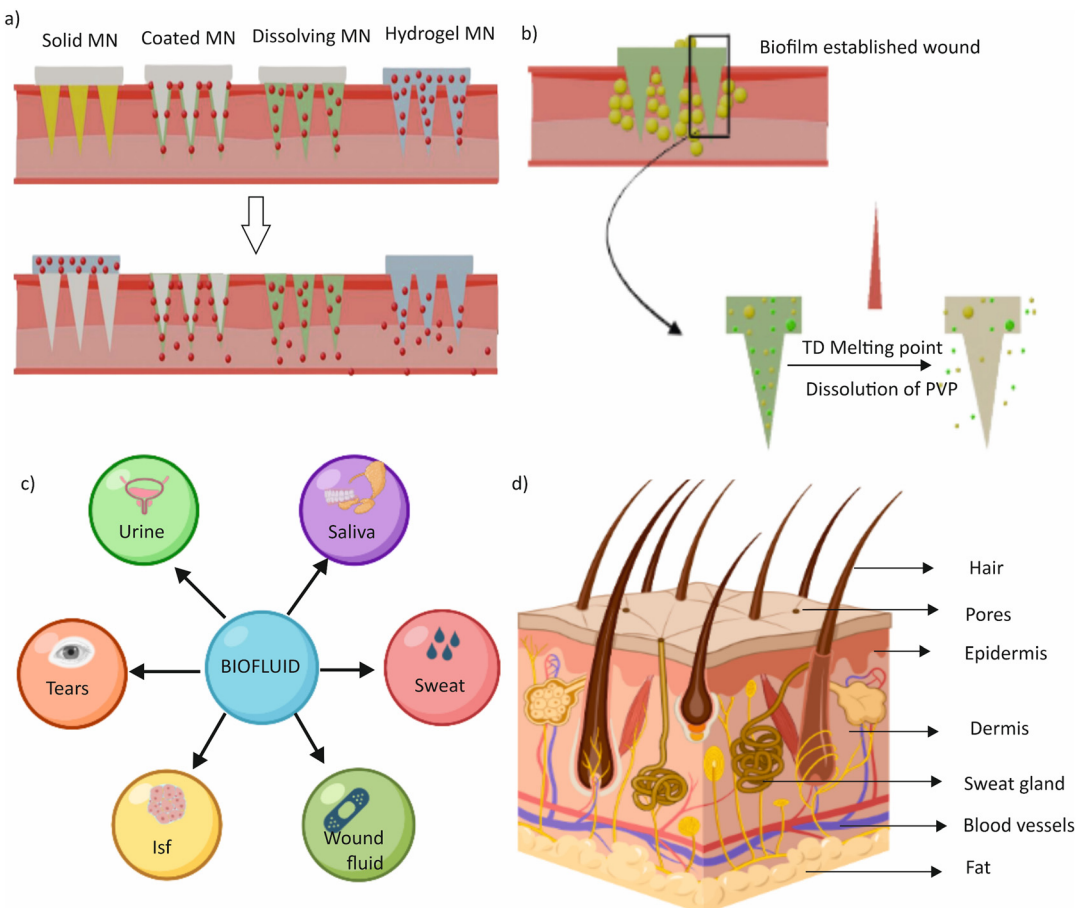


**Fig. 3** a) Schematic diagram showing different types of microneedles. b) Schematic illustration of near-infrared (NIR) light-responsive microneedle patches. c) Schematic presentation of various biofluids. d) Diagrammatic illustration of a cross section of human skin showing sweat glands.

topical cream. Hollow microneedles are used for drug infusion into the skin and can be present in a microfluidic device either singularly or in an array.<sup>90</sup> Coated microneedles are covered with a water-soluble formulation of the drug before administration, which subsequently dissolves into the skin after puncturing.<sup>91</sup> Dissolvable microneedles are made from polymers that dissolve completely after insertion, releasing the therapeutic agent.<sup>92</sup> They are suitable for delivering thermo-sensitive drugs such as proteins and antigens and can be fabricated using micromoulds or *in situ* polymerization of liquid monomers.

Kang *et al.* reported wearable devices utilizing microneedle-based transdermal microfluidics for drug delivery and analyte collection.<sup>93</sup> Hyaluronic acid (HA) is a particularly advantageous material due to its human autologous source, biocompatibility, strong water absorption, and viscoelasticity.<sup>94</sup> The devices were employed for wound healing, targeted therapy, extraction of interstitial skin fluid (ISF), and drug preservation. Luzuriaga *et al.* presented biodegradable 3D printed polymer microneedles for transdermal drug delivery using poly(lactic acid), an FDA-approved biodegradable material.<sup>95</sup> The needles have a tip size as small as 1  $\mu\text{m}$  due to a post-fabrication chemical etching protocol that improved the feature size of the printed parts. Near-infrared (NIR) light-responsive microneedle patches have

also been introduced for the on-demand release of antimicrobial peptides for the treatment of wound biofilms.<sup>96</sup> The patch contains dissolvable poly(vinylpyrrolidone) (PVP) microneedles loaded with IR780 iodide as a photothermal conversion agent and molecularly engineered peptide W379 as an antimicrobial agent. Upon exposure to NIR light, IR780 converts light to heat, causing the phase change material 1-tetradecane (TD) to melt, releasing the loaded W379 peptide from the microneedles into the surrounding regions. The NIR light-responsive microneedle patches can program the release of antimicrobial peptides and show high antibacterial efficacy *in vitro* compared with traditional microneedle patches. Fig. 3b provides a schematic illustration of the above-mentioned microneedle patches.

While microneedles have numerous potential applications,<sup>97,98</sup> only a few products have been so far commercialized. Safety and efficacy considerations are crucial when developing microneedles for delivering small and large molecules. Metallic microneedles may leave metal residues under the skin, leading to various side effects such as irritation, swelling, or discolouration. When microneedles are used repeatedly on the same location of the skin or on areas of the skin with different levels of thickness, the effectiveness of delivering substances through these microneedles can be

influenced. This could lead to problems in how well the substances are absorbed by the body and potentially result in various complications or negative outcomes.<sup>86,89</sup>

### 3. Biofluids

Biofluids are fluids that can be excreted, secreted, or obtained through needle aspiration or as a result of pathological processes in the human body.<sup>99</sup> These fluids contain biochemical components or biomarkers that directly relate to human health conditions.<sup>100</sup> For effective target analysis, it is essential to collect and process biofluids that are typically secreted by the human body. Sweat, saliva, urine, tears, interstitial fluids of the skin, and wound fluids are examples of biofluids commonly analysed by microfluidics-based wearable devices.<sup>32,101</sup> Fig. 3c provides a schematic overview of various biofluids.<sup>102</sup> The collection and analysis of biofluid samples such as blood and urine can be time-consuming and troublesome, when done in a laboratory. However, microfluidics-based wearable devices can help overcome these challenges by ensuring that biofluid collection and analysis are non-invasive, reliable, and accurate.<sup>103</sup> Microfluidic technologies are capable of

collecting biofluids in small amounts, utilizing their advantages on the microscale.<sup>11</sup> This makes microfluidics-based wearable devices highly relevant in the current era.

The following sections provide a discussion of the fundamental composition and physiological and pathological properties of biofluids, as well as the analytes present in them. Additionally, the latest microfluidics-based wearable technologies in this field and the potential for integrating artificial intelligence are addressed. We also discuss the challenges and prospects associated with each biofluid. For ease of further reading, Table 1 shows the typical concentration of analytes in each biofluid along with the associated health hazards. Table 2 shows various existing sensing methods used in wearable devices for different biofluids associated with corresponding limitations.

#### 3.1. Sweat

Sweat is a hypotonic fluid produced by sweat glands as a part of bodily thermoregulation.<sup>104,105</sup> An ordinary human adult can generate 500 to 700 ml of sweat per day.<sup>106</sup> Compared to other bodily secretions, sweat can be collected non-invasively and contains a rich composition of biomarkers such as water,

**Table 1** The concentration of analytes in each biofluid and the associated health hazards of each analyte

Analytes	Concentration	Potential health hazards	Ref.
Glucose	Sweat	0.06 to 0.2 mM	126, 144, 179, 200, 232
	Saliva	0.5 to 1.00 mg/100 ml	
	ISF	60 to 90 mg dL <sup>-1</sup>	
	Urine	25 mg dL <sup>-1</sup>	
	Tears	0.032 mmol L <sup>-1</sup>	
Sodium	Sweat	70 mmol L <sup>-1</sup>	118, 119, 188, 197, 233
	Saliva	8.7 to 24 mEq L <sup>-1</sup>	
	ISF	-135–145 mmol L <sup>-1</sup>	
	Urine	20 mEq L <sup>-1</sup>	
	Tears	120 to 170 mM	
Potassium	Sweat	10 to 50 mmol L <sup>-1</sup>	115, 186, 196, 234
	Saliva	13 to 16 mEq L <sup>-1</sup>	
	ISF	3.97 mM	
	Urine	20 mEq L <sup>-1</sup>	
	Tears	20 mEq L <sup>-1</sup>	
Lactate	Sweat	2 to 20 mmol L <sup>-1</sup>	125, 149, 194, 301, 234
	Saliva	0.1 to 2.5 mM	
	ISF	1 to 2 mM	
	Urine	4.5 to 19.8 mg dL <sup>-1</sup>	
	Tears	1 to 5 mM	
Chloride	Sweat	30–59 mmol L <sup>-1</sup>	117, 120, 189, 223
	Saliva	5 to 40 mmol L <sup>-1</sup>	
	ISF	100–110 mmol L <sup>-1</sup>	
	Urine	110 to 250 mEq	
	Tears	110 and 135 mEq L <sup>-1</sup>	
Uric acid	Sweat	24.5 mmol L <sup>-1</sup>	80, 131, 161
	Saliva	199 ± 27 µmol L <sup>-1</sup>	
	ISF	0.1 to 0.3 mg dL <sup>-1</sup>	
	Urine	250 to 750 mg/24 hours	
	Tears	25–150 µM	
pH	Sweat	6.3	134, 168, 191
	Saliva	6.6 to 7.1	
	ISF	7.35 to 7.45	
	Urine	4.5 to 8	
	Tears	6.5 to 7.6	

Table 2 Sensing methods in wearable devices and their limitations

Sensing method	Biofluid	Analyte	Limitations	Ref.
Amperometry sensors	Blood, interstitial fluid, saliva	Glucose, lactate	<ul style="list-style-type: none"> <li>Sensitive to interfering substances present in the biofluids</li> <li>Accuracy may decrease over time due to electrode fouling</li> </ul>	126, 154, 180, 193
Potentiometric sensors	Blood, sweat, saliva	pH, ions	<ul style="list-style-type: none"> <li>Limited dynamic range</li> <li>May exhibit slower response times compared to other sensor types</li> <li>pH variations in the biofluid may impact sensor performance</li> </ul>	126, 187, 189, 191
Voltammetric sensors	Blood, interstitial fluid	Uric acid, vitamin C	<ul style="list-style-type: none"> <li>Need antifouling strategies</li> <li>Require sophisticated algorithms or analysis techniques for accurate information extraction</li> </ul>	192, 193
Colorimetric sensors	Blood, urine, sweat	pH, glucose, specific ions	<ul style="list-style-type: none"> <li>Limited quantitative analysis</li> <li>Colour changes can be influenced by external factors</li> </ul>	120, 127, 128, 147, 168
Fluorescence sensors	Blood, saliva, urine, interstitial fluid	Proteins, ions, pH	<ul style="list-style-type: none"> <li>Sensitive to environmental conditions</li> <li>Simultaneous detection of multiple analytes is challenging due to spectral overlap</li> </ul>	235, 246, 305

electrolytes (e.g., sodium, potassium, and chloride), metabolites (e.g., glucose and lactate), trace elements, lactic and uric acid, and drugs.<sup>107–109</sup> The abundance of eccrine glands throughout the body makes sweat collection relatively straightforward. Its non-invasive nature and ready availability make sweat a popular easy-to-access sample.<sup>108</sup>

Sweat contains a wealth of information that can be used for diagnosing various ailments and diseases. For instance, the correlation between glucose levels in blood and sweat enabled continuous monitoring of diabetes, while the amount of lactate in perspiration can provide insight into the severity of ischemia associated with certain diseases.<sup>110</sup> Sodium and calcium levels in sweat can be used to identify and diagnose cystic fibrosis in newborns and other related conditions.<sup>111</sup> Furthermore, skin temperature and sweat analysis can provide valuable information on the occurrence and progression of various skin diseases and conditions.<sup>109,112</sup>

Sweat is primarily collected from the eccrine glands; each sweat gland is connected to vascularized tubes that stretch from the dermis to the skin surface. Sweat is expelled onto the skin surface with the assistance of myoepithelial cells.<sup>106,113</sup> There are two primary methods for collecting sweat: the passive approach and the active approach. The passive approach involves physical exercise or thermal stimuli, such as running, cycling, sauna, or skipping, while the active sweat collection method is commonly done through iontophoresis.<sup>114,115</sup> Iontophoresis involves applying a voltage between two electrodes to stimulate a local area of the skin.<sup>109</sup> However, this technique can be uncomfortable and is prone to electrode corrosion.

Compared to other biofluids, sweat has a lower concentration of biomarkers, which makes quantitative analysis challenging. Conventional sweat analysis devices use absorbent pads or fabrics, which require additional design for processing.<sup>1</sup> These methods are also prone to low secretion rates and evaporation challenges. Microfluidics has

emerged as a promising method for preparing and analysing sweat, as microfluidic devices require only a small volume of sweat and can be designed to be portable, low-cost, reusable, and disposable.<sup>108</sup> Microfluidic components in wearable devices allow for transporting sweat in time after its detection, preventing contamination of sweat for subsequent analysis. Microchannels in the devices can drive and collect sweat in a well-designed manner, improving efficiency.<sup>11</sup>

**3.1.1. Wearable microfluidic devices for the analysis of sweat.** Sodium ( $\text{Na}^+$ ) and chloride ( $\text{Cl}^-$ ) ions are the primary ions found in sweat and are commonly used as biomarkers.<sup>116</sup> Normal levels of these ions in sweat are approximately  $70 \text{ mmol L}^{-1}$  ( $\text{Na}^+$ ) and  $55 \text{ mmol L}^{-1}$  ( $\text{Cl}^-$ ), respectively, and are correlated with the sodium levels in the blood. Sweat ducts that carry sweat from the sweat gland to the skin surface can reabsorb or recapture  $\text{Na}^+$  and  $\text{Cl}^-$  ions through ion channels present in the sweat duct epithelium to prevent electrolyte loss.<sup>104</sup> However, cystic fibrosis can affect the functioning of these ion channels and ducts, leading to abnormal regulation of sodium and chloride ions in the blood. This information can be helpful for the diagnosis of cystic fibrosis and for monitoring the effectiveness of medical treatment.<sup>117,118</sup>

Cystic fibrosis is associated with high levels of chloride ions in sweat, making them a crucial indicator of the disease. A potentiometric chloride ion biosensor was developed for the diagnosis and management of cystic fibrosis as explained by Grasta *et al.*<sup>119</sup> The sensor uses ion-sensitive field-effect transistors to detect the presence of chloride ions in sweat. FEM-based modelling, which includes both semiconductors and electrochemistry, is used to develop the sensor. However, these biosensors can be expensive and require calibration, limiting their widespread adoption in clinical settings.

Similarly, Biswas *et al.* reported a novel transdermal patch for cystic fibrosis diagnosis.<sup>120</sup> The patch, which looks like a conventional sticker, absorbs sweat through tiny canals. Pilocarpine, a drug that stimulates sweat production, is

applied to the skin using a mild electric current. The resulting colour change indicates the presence of cystic fibrosis. While this approach is simple and non-invasive, the colorimetric readout can be difficult to interpret in low-light settings.

To address some of these challenges, a soft, epidermal microfluidic device ("sweat sticker") has been designed for the simple and rapid collection and analysis of sweat.<sup>121</sup> Intimate, conformal coupling with the skin supports nearly perfect efficiency in sweat collection without leakage. Real-time image analysis of chloride reagents allows for quantitative assessment of chloride concentrations using a smartphone camera, without requiring extraction of sweat or external analysis. However, the wearable microfluidic technologies and smartphone-based analytics reported here are still in the experimental stage and may require further refinement before they can be widely adopted in clinical settings.

Potassium ( $K^+$ ) is an important electrolyte present in sweat, along with sodium and chloride. Unlike sodium and chloride,  $K^+$  is independent of the sweat generation rate and has a strong correlation with blood concentration.<sup>116</sup> Measuring  $K^+$  levels in sweat can be used as an indicator of

the hydration status, as well as to monitor conditions such as renal disease and dehydration.<sup>122</sup> The normal range of  $K^+$  in sweat is between 10 and 50 mmol L<sup>-1</sup>, but may vary depending on the individual.<sup>123</sup>

Recent advancements in wearable technology have led to the development of devices that can measure  $K^+$  levels in sweat in real-time. One of such devices is the SwEatch platform, which uses ion-sensitive electrodes (ISEs) fabricated and containing either poly(3,4-ethylenedioxothiophene) (PEDOT) or poly(3-octylthiophene-2,5-diyl) (POT) as a conductive polymer transducing component. The microfluidic unit of the device draws sweat from the skin through a passive capillary reaction and brings it into contact with the two electrodes. This technology is mainly focused on sport application and can provide immediate feedback on hydration levels of athletes. Liang *et al.* demonstrated an integrated three-dimensional paper-based microfluidic electrochemical device (3D-PMED) for real-time monitoring of sweat potassium.<sup>124</sup> Fig. 4a shows the schematic illustration of the device with channels, an electrode layer, and a sweat evaporator. The device includes a screen-printed potassium ion-selective sensor on a PET substrate and a paper-based microfluidic pad for sweat collection and

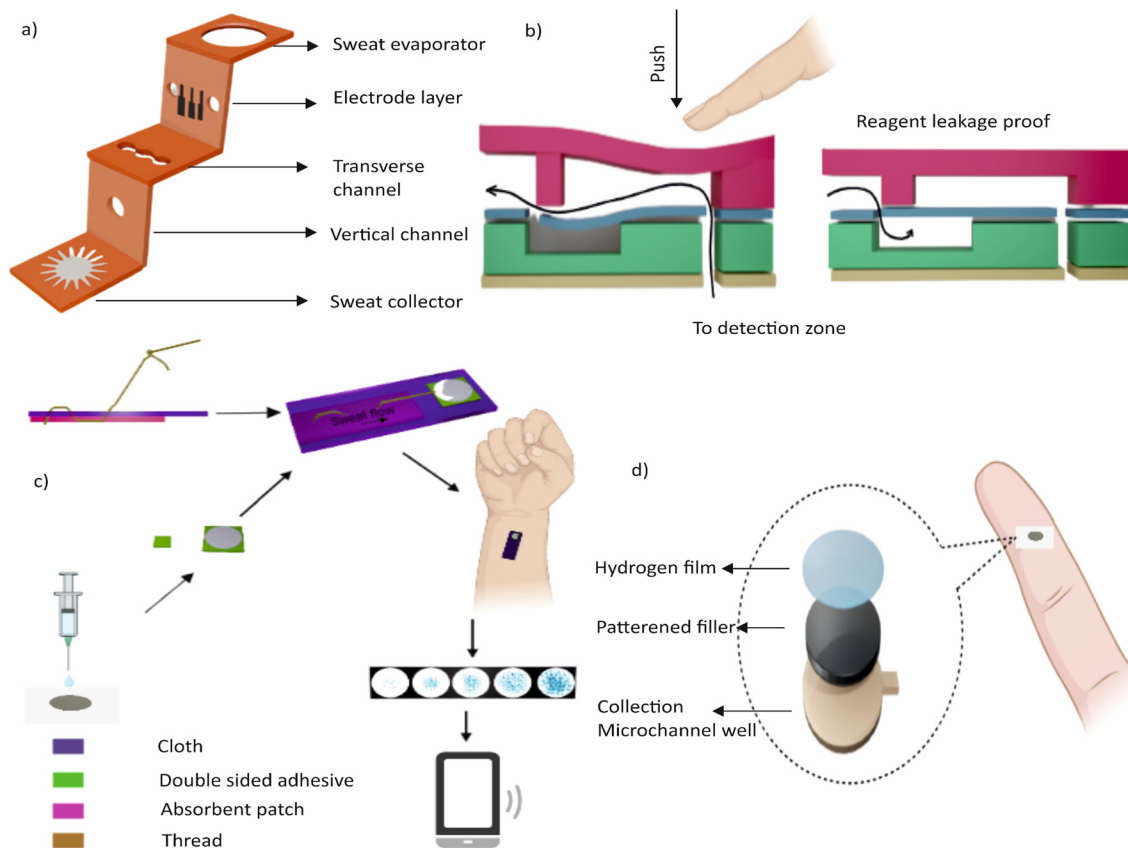


**Fig. 4** a) Schematic illustration of the 3D-PMED having a layered structure with channels, an electrode layer, and a sweat evaporator. A three-electrode sensor is affixed to the electrode layer. b) Schematic drawing of the structure and function of the integrated microfluidic check valve. c) Conceptual diagram of *in situ* monitoring of human sweat glucose in the microfluidic thread/paper-based analytical device ( $\mu$ TPAD) by Xiao *et al.* d) Illustration of a wearable patch for continuous sweat monitoring at rest, which has hydrophilic fillers for rapid sweat uptake into the sensing channel.

detection. The 3D-PMED technology offers a detection range of 1–32 mM and has the potential to address the limitations of existing sweat monitoring methods.

While  $K^+$  as an indicator of the hydration status is a promising marker, there are limitations to this approach. For example, factors affecting the level of  $K^+$  in sweat are exercise, medication, and diet. Additionally, the accuracy of  $K^+$  measurement can be affected by factors such as skin temperature and sweat generation rate. To address these limitations, future research could explore the use of multi-sensor systems that integrate  $K^+$  measurement with other parameters such as skin temperature and sweat rate. Such systems could provide a more comprehensive assessment of an individual's hydration status and help to improve the accuracy of  $K^+$  measurement in sweat.

**Lactate.** Lactate is a hydrophilic metabolite and analyte that is present in sweat. During exercise and muscle activities, glycogen breakdown locally produces lactate in sweat. There is also a correlation with blood lactate levels. Typically, the lactate concentration in sweat ranges from 2 to 20  $\text{mmol L}^{-1}$ . While lactate is primarily used as a potential biomarker for exercise analysis in most wearable devices, lactate sensors are typically integrated with other sensors to provide multiplex and comprehensive health monitoring.

One example is the epidermal patch developed by Sempionatto *et al.*, which allows for the simultaneous monitoring of haemodynamic and metabolic biomarkers.<sup>125</sup> This non-invasive device utilises ultrasonic transducers and electrochemical sensors to monitor blood pressure and heart rate using multiple biomarkers, including lactate. Another example is a continuous sweat monitoring system that is integrated with wireless electronics in the form of wearable glasses.<sup>126</sup> This real-time monitoring system has a chemical sensing platform capable of sensing electrolytes and metabolites in sweat such as lactate and potassium ions. The system includes an amperometry lactate biosensor and a potentiometric ion-selective electrode on the two nose bridge pads of the spectacles, with PET stickers used on the glass nose pads to monitor sweat metabolites and electrolytes. The entire setup is integrated into the arms of the glass for wireless electronic communication.

**Glucose.** Glucose is another crucial substance that is commonly evaluated in sweat. Though it is typically found in blood, glucose can also be detected in sweat, albeit at a much lower concentration. The normal range of glucose in sweat is between 0.06 and 0.2 mM, compared to 3.3 to 17.3 mM in blood. Factors such as diet, exercise, and stress levels can affect the concentration of glucose in sweat. The correlation between glucose in sweat and glucose in the blood is a subject of ongoing research. However, studies have shown that there is a strong correlation between the two in both type 1 and 2 diabetes cases, even during exercise.

The measurement of glucose levels in sweat has potential applications in monitoring diabetic patients and athletes during exercise. There is increasing interest in epidermal wearable devices for tracking sweat glucose. These devices

offer a non-invasive and continuous way of monitoring glucose levels, which could be more convenient for patients compared to traditional blood glucose monitoring systems. Examples of sweat-based glucose monitoring devices include wristwatches, wearable patches, optical instruments, and stretchable tattoos. One of such devices is a microfluidics-based wearable colorimetric sensor designed to detect glucose in sweat demonstrated by Xiao *et al.*<sup>127</sup> Fig. 4b shows the schematic of the device. The sensor consists of five microfluidic channels connected to detection microchambers with a check valve in each channel to prevent the backflow of chemical reagents. The microchambers contain pre-embedded glucose oxidase (GOD)-peroxidase-*o*-dianisidine reagents that sense glucose in sweat. The sensor shows a more sensitive response to glucose than conventional GOD-peroxidase-KI systems and can perform five parallel detections simultaneously. The sensor has a linear range for sweat glucose of 0.1–0.5 mM with a limit of detection of 0.03 mM.

Another wearable device developed for non-invasive, quantitative, and *in situ* monitoring of human sweat glucose is the microfluidic thread/paper-based analytical device ( $\mu$ TPAD) reported by Xiao *et al.*<sup>128</sup> (Fig. 4c). The device contains a cotton thread and functionalized filter paper that achieves high-performance colorimetric sensing of glucose. The  $\mu$ TPAD is integrated with an arm guard to sensitively detect glucose in human sweat, making it a low-cost and easy-to-use wearable device for human sweat analysis. In addition, a soft and flexible wearable sweat epidermal microfluidic device capable of simultaneously stimulating, collecting, and electrochemically analysing sweat was demonstrated by Bolat *et al.*<sup>129</sup> The device integrates an iontophoretic pilocarpine delivery system around the inlet channels of the epidermal polydimethylsiloxane (PDMS) microfluidic device for sweat collection and analysis. The device eliminates the need for intense physical exercise as the freshly generated sweat is naturally pumped into the fluidic inlet. The on-body performance and layout of the device were optimized. The device was evaluated for detecting sweat glucose in several volunteers. Furthermore, the microfluidic monitoring device was integrated with a real-time wireless data transmission system using a flexible printed circuit board conformal with the body surface.

**Uric acid.** Uric acid is a waste product typically excreted in urine, but it can also be found in sweat at a measurable level.<sup>130</sup> Monitoring the levels of uric acid in sweat provides valuable insights into an individual's health status, such as dehydration, increased physical activity, or hyperuricemia.<sup>131</sup> However, the correlation between the levels of uric acid in sweat and blood is not always direct, and the concentration of uric acid can vary depending on the individual even without hyperuricemia.<sup>130,132</sup> Despite these challenges, recent advances in wearable technology have led to the development of microfluidic-based electrochemical and plasmonic sensors for accurate and sensitive detection of uric acid in sweat.

Mogera *et al.* introduced a wearable plasmonic paper-based microfluidic system for continuous and simultaneous quantitative analysis of sweat loss, sweat rate, and metabolites in sweat.<sup>81</sup> Plasmonic sensors based on label-free surface-enhanced Raman spectroscopy (SERS) provide chemical “fingerprint” information for analyte identification, enabling sensitive detection and quantification of uric acid in sweat at physiological and pathological concentrations. Xu *et al.* proposed a wearable microfluidics-based electrochemical sensor incorporating a conducting polymer PEDOT:PSS hydrogel for the accurate and sensitive detection of uric acid in sweat.<sup>133</sup> The prepared flexible sensor shows an ultrahigh sensitivity and a low limit of detection and is capable of detecting uric acid levels in real human sweat samples. These microfluidic devices have promising applications in the construction of high-performance wearable sensors for monitoring biomarkers, metabolites, and nutrients. However, further research is required to fully understand the correlation between the levels of uric acid in sweat and blood.

**Sweat pH.** Sweat pH is one of the key parameters to monitor an individual's health. The pH of human sweat ranges typically between 4.5 and 7.0. The average pH of sweat for a healthy human is 6.3. The pH of sweat is influenced by various factors such as electrolyte concentration and bacterial activity. An imbalance in pH levels can lead to skin disorders and medical conditions. To address this, the National University of Singapore has developed a pH sweat sensor that offers a flexible and highly responsive method of detecting and analysing sweat pH-related issues.<sup>134</sup> The sensor is made of polyaniline polymer, a cost-effective, durable, and flexible material that can change colour based on sweat pH. The sensor can be integrated with smartwatches or pulse oximeters to offer continuous monitoring of sweat pH.

A wearable wristband has been developed for collecting sweat from the skin and has a colour-based pH area for easy readout.<sup>135</sup> Real-time data can be transmitted to smart applications through a Bluetooth interface. Additionally, a wearable patch has been developed for continuous sweat monitoring at rest, which has hydrophilic fillers for rapid sweat uptake into the sensing channel and is integrated with an electrochemical sensor for pH, Cl<sup>-</sup>, and levodopa monitoring.<sup>136</sup> Fig. 4d shows this wearable patch.

In addition to pH, sweat contains a wide range of analytes such as lipophilic molecules, steroid hormones, and legal and illicit drugs like heroin, morphine, and methadone.<sup>101</sup> Sweat analysis has the potential to offer valuable insights into an individual's physical condition and health. Over 800 unique proteins and more than 32 000 endogenous peptides have been discovered in sweat,<sup>137</sup> offering a promising avenue for further research.

**3.1.2. Challenges and outlook.** Sweat analysis with wearable microfluidic devices has demonstrated great potential for non-invasive and continuous monitoring of various biomarkers. These devices allow for real-time data collection, providing insights into the physical condition and health of the wearer. However, several challenges are associated with sweat analysis

and must be addressed to maximize the potential of these devices.

One major challenge is the variation of sweat composition, which can be influenced by factors such as temperature, exercise, and the physiological status. This variation affects the accuracy and reliability of the analysis, especially in cases where sweat is exposed and contaminated. In addition, individual differences and variations in physiological and pathological states, such as gender, diet, and genetics, can further complicate the analysis and interpretation of results.

Another challenge is the limited applications of sweat analysis using microfluidic wearable devices, which are currently restricted to monitoring cystic fibrosis, diabetes, and performance of athletes during exercise. Despite providing valuable information about human physiology through biomarkers, the potential applications of sweat analysis remain restricted. Therefore, further research and development are needed to explore and expand the potential of these devices.

Overall, the challenges associated with sweat analysis using wearable microfluidic devices highlight the need for continued innovation and improvement in this field. Addressing these challenges will be crucial for reaping the full potential of sweat analysis as a non-invasive and continuous monitoring tool for physiological and pathological conditions.

### 3.2. Saliva

Saliva is a readily accessible biofluid produced by three major and numerous minor salivary glands, containing biomarkers similar to sweat.<sup>138</sup> The minor glands produce 10% of total saliva, which contains more blood components, while the major glands, including the parotid, submandibular, and sublingual glands, produce 90% of total saliva. The individual production of saliva is 20%, 65%, and 7–8% for the respective glands.<sup>139</sup> Saliva production varies depending on factors such as time of day, age, gender, taste, and smell stimulus. There are two types of saliva, stimulated and unstimulated. The production rate of saliva is controlled by the sympathetic and parasympathetic nervous systems. The saliva's composition includes hormones, proteins, electrolytes, mucus, enzymes, glycoproteins, inorganic and organic compounds, and antibacterial compounds, with the concentration of these components varying between stimulated and unstimulated saliva.<sup>140</sup>

Saliva plays a crucial role in the human body by aiding in digestion, lubricating the mouth, protecting teeth from decay, and preventing infections.<sup>141</sup> Analysing saliva can provide valuable information about a person's health status, including the diagnosis and monitoring of various diseases such as diabetes, autoimmune diseases, infections, and cancer. It can also be used to monitor drug levels and assess the effects of medication.<sup>142</sup> Salivary analysis is a non-invasive, easy-to-collect, and cost-effective method compared to other biofluids such as blood or urine. Due to its potential

in early disease detection and personalized medicine, the popularity of salivary analysis has increased in recent years.<sup>101</sup>

The concentration of the biomarkers in saliva may vary depending on the individual's physiological and pathological state, which makes it necessary to establish a correlation between salivary biomarkers and data of the human body.<sup>143</sup> The analysis of saliva biomarkers can provide useful information on various physiological and pathological conditions, such as inflammation, hormone levels, oral health, and stress levels. Saliva has also been used in sports medicine to monitor athletes' hydration and electrolyte balance.<sup>144</sup>

**3.2.1. Wearable microfluidic devices for the analysis of saliva.** Saliva has been shown to contain glucose at concentrations lower than those found in blood but with a strong correlation between the two. Typically, the normal glucose level in saliva ranges from 0.5 to 1.00 mg/100 ml, which is insufficient for the growth of microorganisms. Salivary glucose has emerged as a non-invasive alternative to blood for diagnosing and monitoring diabetes mellitus, especially in situations where other biofluids like blood or urine are not easily obtainable, such as with children, the elderly, and critically ill patients.<sup>145</sup>

Several studies have explored the development of wearable salivary biosensors for glucose monitoring. de Castro *et al.* introduced a paper microfluidic device for detecting salivary glucose and nitrate, Fig. 5a.<sup>146</sup> This device consists of two interconnected detection zones through a microfluidic channel and has been integrated into a silicon mouthguard using a 3D-printed holder. However, the device has limitations due to its colorimetric evaluation.<sup>147</sup>

Arakawa *et al.* developed a salivary biosensor that incorporates Pt and Ag/AgCl electrodes on a mouthguard support with an enzyme membrane, Fig. 5b.<sup>148</sup> The electrodes are formed on the polyethylene terephthalate glycol (PETG) surface of the mouthguard, and the Pt working electrode is coated with a glucose oxidase (GOD) membrane. Although the biosensor seamlessly integrates with a glucose sensor and a wireless measurement system, the potential disadvantage of this technology is the form factor of the mouthguard, which may not be a convenient or comfortable option for some users.

García-Carmona *et al.* developed a portable saliva-based sensor for continuous monitoring of glucose levels in infants.<sup>149</sup> The sensor uses a nontoxic polymeric nipple for saliva collection, making it more practical for infants compared to invasive methods or wearable devices. The glucose-oxidase enzyme is immobilized on the electrode using chitosan, and the resulting oxidation of glucose creates detectable changes in current that are read by a Prussian blue electrode transducer. Although the functionality of the sensor was tested in type I diabetic patients and showed comparable results to blood tests, the potential disadvantage of the device is that its response may be affected by changes in temperature and humidity, requiring frequent recalibration to maintain its accuracy over time.

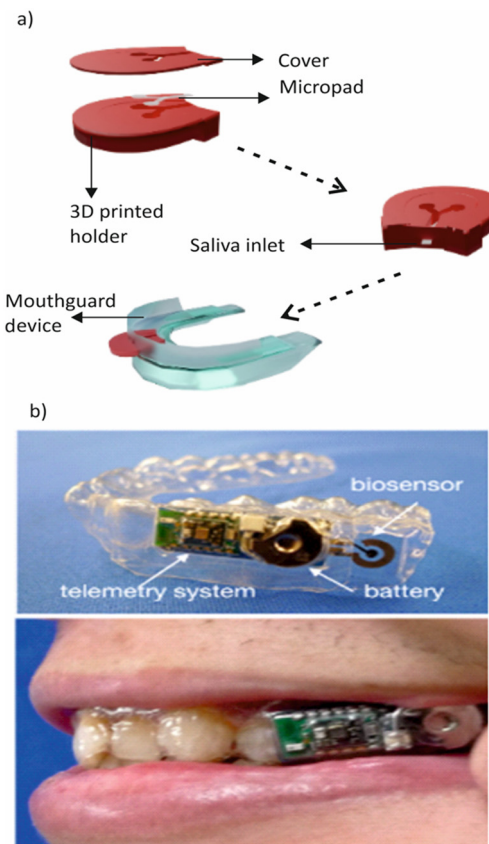


**Fig. 5** a) Conceptual diagram of a 3D-printed paper microfluidic device for detecting salivary glucose and nitrate. b) Schematic representation of a salivary biosensor that incorporates Pt and Ag/AgCl electrodes on a mouthguard support with an enzyme membrane. Reprinted with permission from ref. 143. Copyright 2020, American Chemical Society.

Saliva is a promising biofluid for detecting lactate, a compound that indicates various medical conditions and physical performance.<sup>150</sup> The concentration of lactate in the saliva is correlated with that in the blood, making it a non-invasive and convenient alternative to blood sampling. The normal range of salivary lactate concentration is 0.1 to 2.5 mM, with higher levels indicating metabolic abnormalities or exercise-induced stress.<sup>151</sup>

One potential application of salivary lactate measurement is diabetes management, as lactate and glucose have a close metabolic relationship.<sup>152</sup> Monitoring salivary lactate levels provides insights into glucose metabolism and helps optimize treatment strategies. Additionally, athletes can benefit from salivary lactate measurement as it can help to determine lactate threshold and adjust their training intensity accordingly.<sup>142,153</sup>

Several biosensors have been developed for salivary lactate measurement, including wearable devices that offer real-time monitoring. Kim *et al.* developed a wearable device that uses lactate oxidase immobilized on a polymeric film for amperometry measurement.<sup>154</sup> However, the field of microfluidics-based sensors for salivary lactate is still

underdeveloped. Existing wearable technologies for saliva monitoring can be expensive, complex, and not well-suited for practical use.

Saliva analysis is a promising avenue for detecting various hormones in the body. Cortisol, the primary hormone detected in saliva, has a strong correlation with its concentration in the blood and is commonly studied for stress and anxiety monitoring.<sup>155</sup> Salivary testosterone levels can also be used to study behaviour and sports endocrinology in both males and females, while salivary progesterone levels can be used to monitor menstrual cycles and pregnancy in females. In addition, salivary dihydroxyphenyl glycol and melatonin have also been studied for their potential uses in detecting catecholamine levels and pineal physiology in newborns, respectively.<sup>156–159</sup>

Despite the potential benefits of salivary hormone analysis, there is a lack of wearable devices that can detect these hormones accurately and conveniently in real time. Current devices with microfluidic technology are not flexible or wearable on the human body, and many require additional components for hormone analysis, making them more expensive and inconvenient for users. For instance, while a label-free paper-based electrical biosensor chip has been developed to quantify salivary cortisol at the point-of-care level, it still requires a lab-built, miniaturized PCB for electrical connection and wireless data transmission.<sup>160</sup>

To fully harness the potential of salivary hormone analysis, much research is needed to develop microfluidic wearable devices that can accurately and conveniently detect salivary hormones in real time without additional components. Such devices would enable continuous monitoring of hormone levels in a non-invasive manner, providing valuable insights into the physiological state of the body. Moreover, they would be particularly useful in fields such as sports endocrinology, where monitoring hormone levels can provide valuable information for optimizing training regimens and performance.

Uric acid is an abundant analyte in saliva, offering a non-invasive means of detection. Saliva testing is a useful technique for monitoring hyperuricemia, hypertension, metabolic syndrome, and cardiovascular risks, as there exists a linear relationship between blood and salivary uric acid.<sup>161</sup> A healthy individual has a concentration of  $199 \pm 27 \mu\text{mol L}^{-1}$  uric acid in saliva. Kim *et al.* developed an instrumented mouthguard capable of non-invasively monitoring salivary uric acid levels using an enzyme-modified screen-printed electrode system integrated onto a mouthguard platform along with anatomically-miniaturized instrumentation electronics featuring a potentiometer, a microcontroller, and a Bluetooth Low Energy (BLE) transceiver.<sup>162</sup> However, the device is not wearable because of the requirement of wearing the bulky mouthguard, which may be inconvenient and uncomfortable for some. The absence of microfluidic wearable devices in this field is a significant limitation toward continuous real-time monitoring of analytes such as uric acid.

Saliva contains immunoglobulin A (IgA) and immunoglobulin G (IgG), which are important in fighting pathogens such as

viruses, fungi, bacteria, allergic components and parasite agents.<sup>163</sup> The measurement of these two antibodies is crucial in assessing mucosal humoral immunity and various intestinal issues related to worms.<sup>164</sup> IgA is actively transported into saliva, while IgG enters through passive leakage. Mannoor *et al.* developed an early wearable platform for detecting bacteria using saliva as a sample in 2012.<sup>165</sup> The team used water-soluble silk with printed graphene to transfer it onto bovine tooth enamel, enabling the detection of bacteria even at a single-cell level through self-assembly of antimicrobial peptides on the graphene surface. This resonant-circuit-based device functions without onboard power and could be monitored wirelessly. The team tested the device on *H. pylori*, a bacterium that leads to duodenal ulcers, and demonstrated the detection of a low number of cells in a 1  $\mu\text{L}$  sample, indicating its sensitivity and potential for remote monitoring of pathogenic bacteria. However, the semi-selectivity of the device might limit its application. Furthermore, since the structure and properties of bovine tooth enamel differ from those of human tooth enamel, it might not be ideal for human use as a substrate. In addition, saliva can also be used for detecting human immunodeficiency virus (HIV), hepatitis C virus, and SARS-CoV-2 (COVID-19) virus.<sup>166</sup>

The normal pH level of human saliva is 6.6 to 7.1. Real-time monitoring of pH in saliva would be beneficial to understand the health condition of the oral cavity and digestive system.<sup>167</sup> Matzeu *et al.* developed an edible colorimetric pH sensor.<sup>168</sup> The sensor shows different colours when exposed to saliva with various pH levels, allowing for easy observation of salivary pH levels with the naked eye. The controlled concentration of the pH indicator ensures biosafety and controlled cost. However, the disadvantage of this sensor is its inability to provide continuous and real-time monitoring of the pH changes in saliva, which is crucial for some applications. A wearable device for wireless real-time monitoring of salivary pH in patients has been developed by Mondal *et al.*,<sup>169</sup> which includes a miniaturized battery-less passive transponder. The transponder consists of an RF front end with digital modulation circuitry and sensing electrodes for electrochemical detection and is capable of detecting changes in pH from 4 to 9. The digital circuitry converts sensor data into a bit sequence and provides the digital sensing data over the reflected backscattered signal. Although the sensor demonstrated a sensitivity of 49.5 mV pH<sup>-1</sup>, a potential limitation is the narrow pH range. Nevertheless, this technology has the potential for monitoring pH in soil, food, chemicals, and other areas beyond healthcare.

**3.2.2. Challenges and outlook.** Saliva is a valuable bodily fluid that can provide insight into human physiology, but there are limited options for wearable sensors to monitor it compared to skin. The development of wearable sensors for saliva faces significant challenges, particularly in terms of the form factor and user-friendliness.<sup>153,162</sup> Current devices are bulky and uncomfortable for long-term use, whereas users prefer thin, patch-like or tattoo-like wearables. Integrating 5G technologies and microfluidics into wearables could be a potential solution to these challenges.

Saliva is a complex fluid that contains impurities, such as charged ions, enzymes, and microorganisms, which can interfere with or damage oral wearable sensors.<sup>155,156,167</sup> Despite efforts to improve their reliability, current oral wearable sensors still struggle to meet user demands in this regard.<sup>113</sup> The oral cavity is also home to numerous physiological activities that affect the accuracy of the sensor. Although patch or sticker-like oral cavity devices can help mitigate these issues, their removal and washability for hygiene purposes must also be considered. Nanotechnology and materials science may be leveraged to achieve biocompatibility and avoid toxicity.<sup>170</sup>

Despite the above challenges, wearable devices for analysing saliva are expected to advance to detect viruses like HIV and SARS-CoV-2. Wearable sensors are predicted to play a critical role in disease diagnosis and prevention by integrating with microfluidics and AI, ultimately leading to the diagnosis of future pandemics.

### 3.3. Interstitial fluid (ISF)

Interstitial fluid (ISF) is an increasingly popular biofluid for wearable medical devices due to its accessibility and similarity to blood composition.<sup>171,172</sup> ISF is a colourless fluid found in the spaces between cells, and it can be sampled non-invasively through techniques such as microneedles. ISF is formed by the exchange of fluids and solutes between capillaries and cells through various types of diffusion.<sup>173</sup> The accessibility of ISF makes it ideal for monitoring metabolic disorders, therapy assessments, and organ failure, among other medical conditions.<sup>101</sup>

ISF analysis has been challenging in the past due to the difficulty in collecting and analysing samples. ISF is formed from capillaries, its composition is very similar to that of blood, with the highest correlation among all the biofluids in terms of concentration of analytes.<sup>174</sup> ISF is found in many parts of the body, including the epidermis, around the salivary and sweat glands, and in other tissues. As a result, ISF is accessible through minimally invasive techniques such as microneedles.<sup>175</sup> Recent advances in microfluidic technology have made it possible to develop wearable devices that can monitor ISF in real-time. Microneedle patches emerged as a useful analytical tool to address this information gap. These devices measure glucose levels, electrolytes, and other important biomarkers, providing continuous and non-invasive health monitoring.<sup>176</sup> This breakthrough has the potential to transform medical technology, allowing healthcare providers to obtain valuable information about a patient's health status without invasive procedures. The following section presents details about each analyte, including their concentration in blood and associated disorders, along with the respective wearable devices.

**3.3.1. Wearable microfluidic devices for the analysis of ISF.** Interstitial fluid (ISF) is a biofluid used to measure glucose concentration, especially in individuals with diabetes who need to monitor their blood sugar levels regularly.<sup>177</sup> Continuous glucose monitoring is essential for people with diabetes to

maintain optimal glucose levels and avoid complications.<sup>178</sup> Although blood glucose and ISF glucose levels are closely related, ISF glucose levels are typically 10 to 15% lower. While fasting, the average blood glucose level ranges between 70 and 100 mg dL<sup>-1</sup>, whereas in ISF, it ranges between 60 and 90 mg dL<sup>-1</sup>.<sup>179</sup>

Traditionally, measuring blood glucose levels requires a needle inserted into a vein or a finger prick, which can be uncomfortable and painful. Wearable devices that use ISF for continuous glucose monitoring are more practical and less intrusive for diabetic individuals who require frequent glucose monitoring. Takeuchi *et al.* developed a microfluidic chip with porous microneedles (MNs) to collect ISF.<sup>176</sup> Fig. 6a

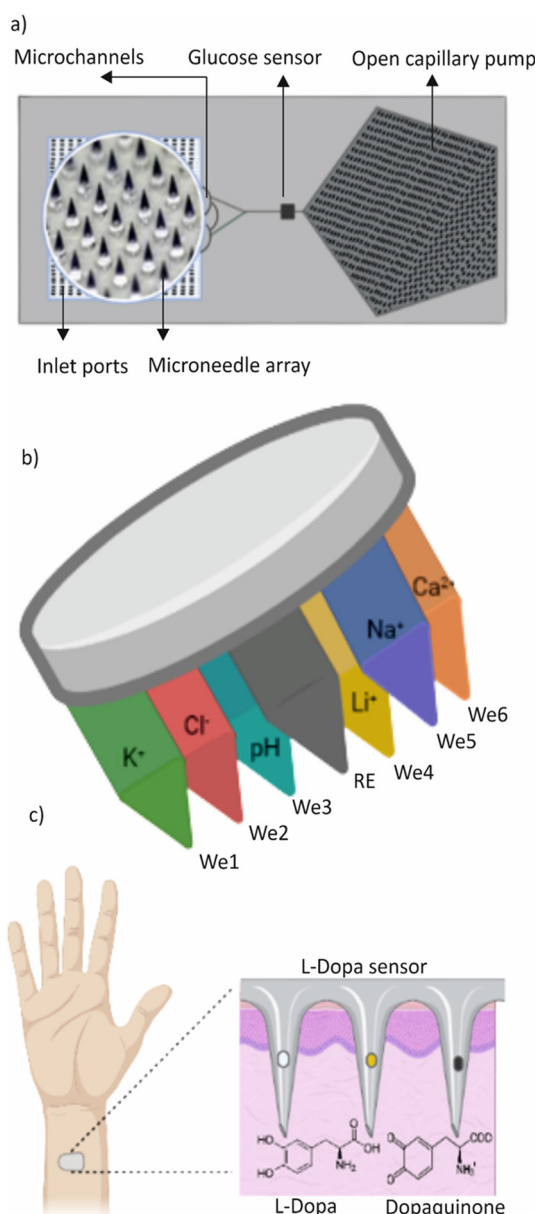


Fig. 6 a) Conceptual illustration of a microfluidic chip with porous microneedles (MNs) to collect ISF. b) Graphical representation of the MIMN patch. c) Microneedle sensing platform for continuous and minimally invasive monitoring of levodopa.

shows a conceptual illustration of the microfluidic chip with porous microneedles. The microfluidic chip with an interface for the MN array enabled liquid flow through the entire microfluidic structure. The team also designed a  $\text{Na}^+$  sensor and correction model to eliminate the effect of individual differences that cause fluctuations in the amount of ISF extracted. Additionally, they designed an electrochemical sensor with a 3D nanostructured working electrode surface to enable precise *in situ* glucose measurement.

A skin-worn, disposable, wireless electrochemical biosensor for extended non-invasive monitoring of glucose in interstitial fluid (ISF) has been developed, integrating a screen-printed iontophoretic electrode system for ISF extraction by reverse iontophoresis (RI), a printed three-electrode amperometry glucose biosensor, and an electronic interface for control and wireless communication.<sup>180</sup> However, it is important to note that prolonged wear of these devices may cause skin irritation or allergic reactions, and frequent replacement of disposable components may increase the overall cost of long-term operation.

Currently, several options for continuous glucose monitoring using ISF are available in the market, including Freestyle Libre by Abbott,<sup>181</sup> Dexcom G6 by Dexcom,<sup>182</sup> Eversense by Senseonics,<sup>183</sup> and Guardian Connect by Medtronic.<sup>184</sup> These diagnostic systems use a small needle-like sensor and transmitter to measure glucose levels in the subcutaneous interstitial space. Some of these systems, such as MiniMed<sup>185</sup> and Paradigm Revel by Medtronic and t:slim X2 by Tandem, are integrated with insulin pumps that can adjust insulin doses automatically based on glucose levels.

Potassium is one of the electrolytes found in ISF along with sodium, chloride and bicarbonates. As mentioned in sweat and saliva, the concentration of electrolytes such as potassium is important for the well-being of the human body.<sup>186</sup> Potassium was found to be 4.37 mM in plasma and 3.97 mM in ISF. A new analytical all-solid-state platform for intradermal potentiometric detection of potassium in interstitial fluid is presented by Parrilla *et al.*<sup>187</sup> This epidermal patch showed good analytical performance and the cell also demonstrated fast response time, selectivity, and reproducibility, making it appropriate for potassium analysis in ISF at both clinical and harmful levels. Miller *et al.* developed a microfluidic-microneedle platform that combines a hollow microneedle with a microfluidic chip to analyse the potassium content in interstitial fluid.<sup>188</sup> To extract fluid through a channel, this system additionally contains a solid-state ion-selective electrode downstream.

Electrolytes such as sodium, chloride, and calcium are essential for maintaining human health, along with potassium. Therefore, it is imperative to monitor their levels throughout the body. Microneedle sensors present a promising avenue for decentralized clinical analyses, allowing for real-time, on-body monitoring of multiple ions simultaneously.

To this end, Molinero-Fernández *et al.* demonstrated the potential of membrane-based microneedles for achieving transdermal multiplexed tracing of pH,  $\text{Na}^+$ ,  $\text{K}^+$ ,  $\text{Ca}^{2+}$ ,  $\text{Li}^+$ ,

and  $\text{Cl}^-$ .<sup>189</sup> Fig. 6b shows a graphical representation of the device. The device features an array of seven solid microneedles, externally modified to provide six indicator electrodes – each selective for a different ion – and a common reference electrode, all integrated into a wearable patch that can be read in potentiometric mode. The accuracy is assessed by benchmarking with gold standard techniques used to characterize collected dermal fluid, blood, and serum. The ability to detect multiple ions simultaneously is relevant for a more comprehensive and reliable assessment of the clinical status of a subject concerning electrolyte disorders and other related conditions.

Another system is a minimally invasive micro-needle-based potentiometric sensing system for continuous monitoring of  $\text{Na}^+$  and  $\text{K}^+$  levels in the interstitial fluid (ISF) of the skin.<sup>189</sup> Li *et al.* designed this system with a miniaturized stainless steel hollow microneedle to prevent delamination and a set of microneedle electrodes for multiple monitoring. However, the accuracy of the measurements is affected by factors such as tissue heterogeneity, depth of insertion, and calibration difficulties. Thus, it is crucial to conduct a thorough evaluation and verification of the accuracy and dependability of these systems before employing them for clinical purposes.

Maintaining the pH level of interstitial fluid (ISF) is crucial for the proper functioning of cells.<sup>190</sup> The pH levels in the blood and ISF are closely related to each other, and any changes in the blood pH level reflect in the ISF pH level. Normal ISF pH ranges between 7.35 and 7.45 levels.<sup>191</sup> However, if the pH level becomes too acidic or alkaline, it can negatively affect cell functions such as cell division and protein synthesis. Therefore, it is important to monitor and maintain the pH level of ISF. García-Guzmán *et al.* developed microneedle (MN) potentiometric sensors for pH transdermal measurements.<sup>191</sup> The initial assessment of the MN sensors demonstrated good analytical performance with a response range of 8.5 to 5.0 and a fast response time in both buffer media and artificial interstitial fluid (ISF). The MN sensors were also evaluated for their ability to resist skin insertions in *ex vivo* setups using animal skins. Researchers are currently in the early stages of studying ISF pH and there are only a few wearable technologies available that can monitor pH levels *in vivo*.

ISF-based monitoring of therapeutic and illicit drugs is an area of growing interest. Research has demonstrated a strong correlation between blood and concentrations of small drug molecules in ISF, making ISF a potential alternative for therapeutic drug monitoring.<sup>101</sup> In a recent research study, Mishra *et al.* introduced a wearable microneedle sensor array capable of continuous electrochemical detection of opioid and organophosphate nerve agents on a single patch platform. The sensor array utilizes unmodified and organophosphorus hydrolase (OPH), enzyme-modified carbon paste (CP), and microneedle electrodes for square wave voltammetric (SWV) detection of fentanyl and nerve agent targets, respectively.<sup>192</sup> The management of Parkinson's disease can be challenging, as the effectiveness of the most commonly used medication,

levodopa, is currently assessed based on the patient's self-report of symptoms. Goud *et al.* developed a new microneedle sensing platform for continuous and minimally invasive monitoring of levodopa.<sup>193</sup> Fig. 6c shows the schematic illustration of the levodopa sensing device. The platform uses multiple microneedles on a single sensor array patch to simultaneously and independently detect levodopa through enzymatic-amperometry and nonenzymatic voltammetric methods. This technology has the potential to improve the monitoring and detection of drugs of abuse, as well as the exposure to chemical weapons in military and civilian settings. However, current studies in this area are limited.

**3.3.2. Challenges and outlook.** Wearable devices that use interstitial fluid (ISF) have gained popularity for continuous glucose monitoring and drug delivery. However, these devices face various challenges such as slow extraction time, low extraction volume, and limited options for analyte analysis, which affect the accuracy and reliability of the data.<sup>101</sup> Glucose measurement in ISF is particularly delayed by 20–35 minutes due to the slow transport rate of glucose molecules, taking up to 1 mm to travel.<sup>194</sup> As such, an improved sensing platform is necessary to reduce measurement delays. Although ISF contains many analytes, including hormones and electrolytes, wearable devices for monitoring these markers have yet to be introduced in the market. Furthermore, there have been concerns regarding device safety due to reported cases of skin burning, allergic reactions, and scarring when inserting or placing new sensors.

To overcome these challenges, researchers are exploring the use of biodegradable and non-toxic materials in designing micro-needles for ISF extraction. They are also seeking to improve the durability and reusability of the devices to minimize frequent skin penetration. Incorporating multiplexed sensors into the device to measure multiple analytes, including glucose, hormones, and electrolytes, is another solution to broaden the scope of monitoring and provide more comprehensive data. Microfluidic technology combined with ISF detection can address most of these challenges and lead to significant progress in this field.

#### 3.4. Tears

Tears are a clear, watery fluid that is secreted by the lacrimal glands, conjunctival goblet cells, or para lacrimal glands.<sup>195</sup> Tears serve the purpose of lubricating and sterilizing the eyes and contain various components such as lysozyme, immunoglobulin, sugar, and inorganic salts, including numerous salts, proteins, enzymes, and lipids.<sup>196</sup> Tears play an essential role in maintaining an individual's health, and a relationship exists between the concentration of glucose, sodium, potassium, and other analytes in blood and tears.<sup>197</sup> Changes in the chemical composition of tears can predict or diagnose various health conditions or diseases, making it a valuable diagnostic tool.<sup>198</sup> A significant breakthrough in tear analysis is its role in detecting breast cancer.<sup>199</sup> Furthermore, changes in tear composition can predict diseases, such as

diabetes and ocular diseases. Tear glucose concentration can also be used in the adjuvant treatment of diabetes.<sup>200</sup>

Since tears are similar to sweat, they can be used for therapeutic drug monitoring. Drugs such as acetaminophen, lithium, anticonvulsants, methotrexate, minocycline, etc. can be analysed using tears.<sup>201</sup> In addition, tears have unique merits for diagnostic purposes. Tears can be collected in a non-invasive manner, which is especially important for patients, who may be uncomfortable with drawing blood or other invasive procedures.<sup>197</sup> Tear collection can also be performed quickly and easily, making it a practical and convenient method for screening and monitoring diseases. Moreover, tears for diagnosis are an emerging research field, and researchers are exploring tear biomarkers for a variety of applications, including the diagnosis and monitoring of cancer, infectious diseases, and neurodegenerative disorders. The following section discusses in detail each analyte in tears, including the corresponding concentration in blood and associated disorders, along with the respective wearable devices and challenges.

**3.4.1. Wearable microfluidic devices for the analysis of tears.** Glucose is one of the primary analytes that can be measured in tears for diagnostic purposes, including continuous monitoring of glucose levels in diabetic patients.<sup>202</sup> Wearable devices that incorporate microfluidics have shown promise for monitoring tear glucose levels in a non-invasive and continuous manner. These devices typically use a small sensor that is placed on the eye, which is then connected to a wearable device that analyses the tear fluid and measures glucose levels. Kudo *et al.* developed a wearable glucose sensor for detecting glucose in tears that uses functional polymers with soft-MEMS techniques.<sup>203</sup> The device is a strip-based sensor that immobilizes glucose oxidase on a flexible hydrogen peroxide electrode. However, applying the strip over the eye may be difficult for some individuals and can irritate if misplaced. In contrast, Chu *et al.* reported a soft contact-lens biosensor for non-invasive biomonitoring of tear fluids, Fig. 7a.<sup>204</sup> This biosensor has an enzyme-immobilized electrode on the surface of a PDMS contact lens and shows a strong correlation between the output current and glucose concentration. Yang *et al.* also developed a flexible, wearable microfluidic contact lens with capillary networks for tear diagnostics, Fig. 7b.<sup>205</sup> The lens allows tears to flow through capillary networks and reservoirs, where chemical substrates respond to biomarkers in the tears by changing colour. The concentration range of the biomarkers can be obtained by taking pictures and reading the red-green-blue (RGB) values in the photos using an external device. The lens was demonstrated to be reliable and convenient to use through *in vitro* tests using an artificial microfluidic hydrogel eyeball device.

Other than glucose, monitoring the intraocular pressure (IOP) is crucial for maintaining good eye health as it aids in the detection and management of various eye disorders such as glaucoma,<sup>206</sup> ocular hypertension, and other related conditions. IOP is the pressure inside the eye that is influenced

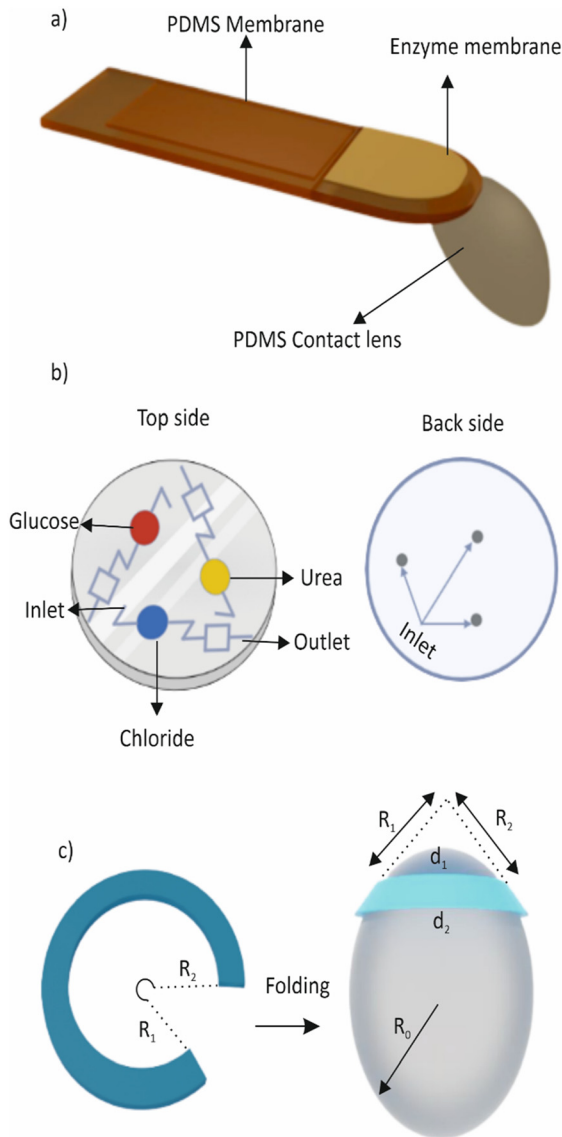


**Fig. 7** a) Structure of the SCL biosensor on the surface of a PDMS contact lens. b) Schematic diagram of the microfluidic contact lens. c) Schematic illustration of folding of the 2D planar notched ring into a 3D spherical ring.

by the equilibrium between the production and drainage of fluid in the eye.<sup>207</sup> Elevated IOP can result in damage to the optic nerve, causing vision loss or blindness. The conventional method of measuring IOP involves using tonometry to measure the pressure on the eye's surface.<sup>208</sup> However, this method has some limitations, such as being uncomfortable for patients and being influenced by the corneal thickness and other eye conditions. Tear-analysing biosensors, on the other hand, are a promising technology that offers a non-invasive and potentially more precise method of IOP measurement.<sup>209</sup> These biosensors detect changes in specific proteins and biomarkers found in tears that are correlated with changes in IOP.<sup>210</sup> As a result, tear-analysed biosensors have the potential to provide an accurate and convenient way of monitoring IOP, particularly for individuals with glaucoma or ocular hypertension who need

regular IOP measurements.<sup>211</sup> Yang *et al.* developed a microfluidic contact lens with a notched-ring structure that monitors intraocular pressure continuously. The lens employs a folding technique that enables the transformation of a planar microchannel from 2D to 3D.<sup>212</sup> Fig. 7c provides a conceptual illustration of the device. To ensure high sensitivity, the folding method is combined with an ultra-sensitive serpentine microchannel in a notched-ring configuration. An *et al.* reported a microfluidic contact lens sensor, which has the potential to continuously monitor intraocular pressure without the need for a power source or invasive procedures.<sup>213</sup> The sensor consists of a micropatterned soft-elastomer sensing layer and a hard plastic reference layer. The device includes an annular sensing chamber filled with dyed liquid and a sensing microchannel that serves as the IOP transducer. When a pressure is applied, the deformation of the sensing layer causes a change in the volume of the sensing chamber, resulting in a displacement of the dyed liquid's interface in the sensing channel. This displacement can be optically observed using a smartphone camera, providing a non-invasive means for monitoring IOP.

A common problem for contact lens wearers is contact lens-induced dry eye (CLIDE), which occurs due to reduced tear volume, tear film instability, and increased tear osmolarity leading to inflammation and discomfort. Zhu *et al.* addressed this issue by developing an eye-blink mimicking system using a microfluidic hydrogel with integrated microchannels.<sup>214</sup> Their *in vitro* study demonstrated that the system could enhance tear transport from the pre-lens tear film to the post-lens tear film by simulating the motion of an artificial eyelid in a pressure range similar to that of human eyelid pressure. The microchannels were made of poly(2-hydroxyethyl methacrylate) (poly(HEMA)). This study provides a proof of concept for the potential of the system to alleviate CLIDE.

Tear devices demonstrated utility beyond monitoring ocular health by enabling drug detection and delivery. The presence of various biomarkers and small molecules in tears makes them a suitable medium for detecting drugs in the body. Additionally, tears have been explored as a non-invasive means for drug delivery, which offers the advantages of bypassing the gastrointestinal and hepatic first-pass metabolism and yielding a more rapid onset of action. In a study by Sempionatto *et al.*, a wearable platform for tear bioelectronics was developed.<sup>215</sup> The platform integrates a microfluidic electrochemical detector into the nose-bridge pad of eyeglasses to monitor key tear biomarkers non-invasively. The biosensing fluidic system uses alcohol-oxidase (AOx) to collect and measure alcohol in real time from stimulated tears, making it the first wearable platform for tear alcohol monitoring. The platform is placed outside the eye region, addressing the limitations of sensor systems that require direct contact with the eye, such as contact lens. The wireless electronic circuitry is integrated into the eyeglasses frame, making it fully portable, convenient, and fashionable to use.

**3.4.2. Challenges and outlook.** Tear-based wearable devices have demonstrated great potential for personalized

health monitoring, with the ability to detect various biomarkers and small molecules in tears. These devices are also cost-effective. Tear analysing wearable devices are virtually invisible, making the users more comfortable while wearing them. This is particularly advantageous for people who may feel self-conscious about wearing a visible device for monitoring their health. However, challenges such as variability in tear composition, sample collection, and interference from other substances need to be addressed. Diagnosis during the production of reflex tears (tears produced by emotional or mechanical stimulation) is also a considerable issue. While a lot of research has been focused on developing tear-based wearable devices for glucose monitoring, there is also great potential for detecting drugs and other small molecules in tears. However, compared to glucose monitoring, the development of devices for drug detection is still in its infancy, and currently only a few devices are available. One of the challenges in developing such devices is ensuring that the sensors are specific and sensitive enough to detect the target molecules in a complex mixture like tears. Incorporating microfluidic systems, developing specific biosensors for multiple analytes, and optimizing the design for user comfort and convenience can be a solution. Additionally, advances in miniaturization, electronic interfaces, and power sources are expected to improve the functionality of tear-based wearable devices. Comfort and easy material selection are important factors, with patches underlying the eye being a reasonable solution for those who find contact lenses invasive.<sup>216</sup>

### 3.5. Urine

Urine is a complex and dynamic biofluid that contains a variety of chemical and biological analytes, including glucose, electrolytes, and hormones. The information provided by these analytes can be invaluable for monitoring an individual's health and detecting the presence of diseases or imbalances in the body.<sup>217</sup> In addition, when a drug is consumed, it is metabolized by the body and excreted through urine. Therefore, urine can be analysed to identify the presence of drugs or their metabolites.<sup>201</sup> Due to its non-invasive and painless collection process, as well as its abundance, urine is an attractive biofluid for wearable devices.

Urinalysis is a technique that has been used for decades to analyse urine, and it involves examining the physical, chemical, and microscopic properties of the sample. Traditional methods of urinalysis include a urine culture, microscopy, and dipstick tests, which can provide information on the presence of bacteria, cells, proteins, and other substances.<sup>218</sup> However, these methods have their limitations, including the need for subjective interpretation and the potential for inaccuracies in test results.

Emerging technologies such as biosensing and microfluidics have the potential to overcome these limitations and improve the accuracy and precision of urinalysis for

wearable devices.<sup>217</sup> Biosensing technologies involve biological receptors such as enzymes or antibodies to detect specific analytes in urine.<sup>219</sup> Microfluidic technologies, on the other hand, involve the manipulation of small volumes of urine through microchannels and microreactors to perform analyses. A well-known application of microfluidics in urine is the use of paper-based devices for home pregnancy tests. These tests detect the concentration of the human chorionic gonadotropin (hCG) hormone in urine, which is a reliable indicator of pregnancy.<sup>220</sup> Overall, the use of urine as a biofluid in wearable devices has significant potential for improving health outcomes by enabling real-time monitoring and early detection of diseases. While there are limitations to current urinalysis techniques, ongoing advancements in biosensing, microfluidics, and alternative specimen collection methods are paving the way for improved analysis of this valuable biofluid.

**3.5.1. Wearable microfluidic devices for the analysis of urine.** Urine is rich in analytes. Glucose is one of them. The level of glucose in urine is correlated to blood glucose levels.<sup>221</sup> Normally, the kidneys filter out excess glucose in blood and return it to circulation. However, if blood glucose levels are consistently high, the kidneys may not be able to reabsorb all excess glucose, which then will be excreted in urine. Therefore, the presence of glucose in urine can indicate elevated blood glucose levels, which can be a sign of diabetes or other health conditions. Glucose levels in urine may not always correlate directly with blood glucose levels. Hydration and kidney function may also affect urine glucose levels.<sup>222</sup>

Sodium and potassium are two electrolytes that are commonly measured in urine. The balance of sodium and potassium in the body is important for the regulation of blood pressure and fluid balance.<sup>223</sup> Typically, the kidneys regulate the amount of sodium and potassium excreted in urine to maintain a healthy balance in the body. However, certain medical conditions or medications can cause imbalances in sodium and potassium levels in urine, which can be determined through urine analysis. Urine also contains various hormones that can provide valuable information about a person's health.<sup>224</sup> As mentioned earlier, human chorionic gonadotropin (hCG) is a hormone produced during pregnancy,<sup>220</sup> and its presence in urine can confirm pregnancy. Similarly, luteinizing hormone (LH) and follicle-stimulating hormone (FSH) are hormones that are involved in reproductive health, and their levels in urine can be used to monitor fertility.<sup>225,226</sup> Cortisol, which is a stress hormone, and aldosterone, which regulates salt and water balance in the body, can also be detected in urine.<sup>227,228</sup>

Despite the presence of valuable analytes in urine, there are few wearable devices capable of detecting them. While portable urine analysis devices do exist,<sup>229–233</sup> the number of continuous monitoring devices utilizing microfluidic technology is limited. Li *et al.* developed a flexible electrode array that can detect various biomarkers such as potassium ions, sodium ions, hydrogen peroxide, uric acid, and glucose, which are indicative of certain conditions, in urine

samples.<sup>234</sup> The array, which is about the size of a U.S. quarter, was connected to a circuit board with a Bluetooth module and a lithium-ion battery power source. When exposed to urine samples from volunteers, the device performed comparably to a commercial urine test system. The team then incorporated the array into a diaper and found that it could detect the biomarkers in the presence of urine. However, it should be noted that in a real-time setting, where dry diapers gradually become saturated with urine, the electrode array would require multiple measurements to obtain stable readings. Couto *et al.* introduced a microfluidic paper-based device that enables the screening and analysis of multiple biomarkers from urine samples on diapers.<sup>37</sup> The device allows for testing five different biomarkers with the same sample by distributing the urine sample into multiple spatially segregated regions through capillary action, without the need for external pumps. The device includes a “self-locking” mechanism that closes the sample inlet in approximately four minutes to prevent contamination and continuous entrance of fluids. Moreover, the device provides comfort by maintaining a total thickness of 5.3 mm.

Another device was reported by Cho *et al.* A microfluidic paper analytical device ( $\mu$ PAD) was created to detect urinary tract infections (UTIs) caused by *E. coli* and sexually transmitted diseases (STDs) caused by *Neisseria gonorrhoeae*.<sup>235</sup> The device consisted of paper microfluidic channels, with anti-*E. coli* or anti-*N. gonorrhoeae* antibodies conjugated to submicron particles, preloaded and dried in the centre of each channel. Undiluted human urine samples spiked with *E. coli* or *N. gonorrhoeae* were mixed with 1% Tween 80 for 5 minutes before being introduced into the  $\mu$ PAD, which then flowed through the channel *via* capillary force. The  $\mu$ PAD successfully filtered out urobilin, which is responsible for the yellow colour and green fluorescence of urine, reducing false-positive signals. Antibody-conjugated particles were then detected by angle-specific Mie scattering, which was quantified using a smartphone camera as a detector. The entire  $\mu$ PAD assay took less than 30 seconds to complete. However, the performance in detecting two specific pathogens in urine samples and the effectiveness for detecting other biomarkers or conditions may vary.

**3.5.2. Challenges and outlook.** Urine as a biofluid in wearable devices requires careful consideration of sample collection, storage, and analysis due to its discrete volume collection and varying composition. Although urine can be used for wearable devices, it is not a common or practical approach because it is not continuously produced like other biofluids such as blood, sweat, or interstitial fluid.<sup>236</sup> Its challenging composition containing waste products and bacteria that can interfere with sensor measurements makes urine difficult to work with. The collection, storage, and handling of urine samples can introduce additional uncertainties.

Moreover, urine is not easily accessible for continuous monitoring using wearable devices, as traditional methods for point-of-care urinalysis such as dipstick tests and microscopy

are often inaccurate and time-consuming. Developing more affordable and accessible diagnostic solutions, such as combining electrochemical biosensors with microfluidics, could greatly improve access to urinalysis and enable earlier detection and diagnosis of diseases. Microfluidic biosensors could detect even low levels of biomarkers in urine and can lead to earlier cancer diagnosis and improved monitoring of chronic diseases, giving an increasing understanding of the pathophysiology of various diseases. However, the success of these devices requires further research and validation of reference concentrations of biomarkers in urine.

### 3.6. Wound fluid

Wound fluid is a biofluid that is produced by the body in response to an injury. Wound fluid plays an important role in the wound-healing process. It is composed of a complex mixture of water, electrolytes, proteins, and cellular components. Wound fluid can be analysed to gain insight into the wound healing process and to monitor the effectiveness of treatments.<sup>237</sup> It helps to remove debris, bacteria, and other foreign particles from the wound site, and it provides a moist environment that is necessary for tissue repair and regeneration. Additionally, wound fluid contains growth factors and cytokines.<sup>238</sup> The presence of certain cytokines in wound fluid can indicate the presence of inflammation or infection and can provide information about the repair and regeneration of the tissues. Analysing the composition of wound fluid will help to choose the suitable dressing technique, the need for antibiotics, *etc.* The exact composition of wound fluid can vary depending on the type and stage of the wound.<sup>239</sup>

Conventional wound dressing involves several steps, beginning with the use of a saline solution or wound cleanser to remove debris and bacteria from the wound.<sup>240</sup> Next, dead tissue may be removed using surgical debridement or debriding agents. Based on the wound type and stage, an appropriate dressing is selected and applied to the wound to promote healing and protect it from further injury. This dressing is typically changed every few days or as directed by a healthcare provider. To supplement the dressing, additional treatments such as antibiotics or growth factors may be used, and the dressing is secured with bandages or tape to maintain a sterile environment. While conventional wound dressing is still commonly used, newer technologies such as smart bandages and microfluidics-based devices offer additional benefits for wound healing. Microfluidics-based devices for wound healing have advantages over traditional wound healing methods and dressing techniques.<sup>241</sup> These devices can deliver drugs in a targeted and controlled manner, monitor wound parameters in real time, can be customized to individual patient needs, reduce the risk of infection, and promote faster healing.

The following section provides insights into various analytes found in wound fluid, as well as their relevance in smart wearable devices and bandages for wound healing. The

section also addresses some of the challenges associated with these devices.

**3.6.1. Wearable microfluidic devices for the analysis of wound fluid.** Wound fluid contains various biochemical molecules and parameters such as C-reactive protein, pH, glucose, uric acid, *etc.* As mentioned in the previous sections, these analytes have a dynamic balance in the normal skin. When an injury occurs, the healthy balance of these analytes will get disturbed and the corresponding changes can provide reliable information for evaluating wound healing. Acute-phase proteins such as C-reactive protein (CRP) are produced by the liver in response to inflammation or infection in the body.<sup>242</sup> When there is an infection in a wound, the concentration of CRP in the blood and local tissue increases. As the infection is resolved, the concentration of CRP in the blood and local tissue typically decreases. CRP can be a useful marker for assessing the presence and severity of wound infections.<sup>241,243</sup> The pH of chronic wounds is a crucial parameter for determining their condition and potential for infection. Generally, a healthy wound has a pH that is slightly acidic ranging between 5.5 and 6.5. However, if the wound becomes infected, bacterial enzymes can break down the surrounding tissue, leading to a more alkaline pH. This shift in pH indicates that the wound is deteriorating, and may require more extensive treatment. Thus, it is important to monitor the pH of chronic wounds to identify those that are at a higher risk of infection and require immediate attention. Mostafalu *et al.* developed a smart and flexible wound dressing that integrates temperature and pH sensors into the bandages, enabling real-time monitoring of the wound healing status.<sup>244</sup> Additionally, the dressing features a drug-releasing system that is responsive to stimuli and comprises a hydrogel that contains thermo-responsive drug carriers, as well as an electronically controlled flexible heater that releases drugs on demand.

The wound dressing also includes a microcontroller that processes the data obtained from the sensors and programs the drug release protocol for personalized treatment. This technology has the potential to revolutionize wound care by allowing for timely and individualized treatment to promote faster healing and improved outcomes. P. Rajput *et al.* developed a prototype of a smart bandage and tested it for its effectiveness in accelerating wound healing.<sup>245</sup> It is capable of monitoring the wound status using pH and moisture sensors. The smart bandage consists of various components such as microchannels, electroosmotic mixers, drug reservoirs that release medication in response to heat stimuli, a DC motor mechanism, a porous material, and small sinks to collect used drugs. A recent study involved the development of a smart wound dressing using a hydrogel that can detect bacterial infections by monitoring pH changes.<sup>246</sup> This is done through a fluorescence resonance energy transfer (FRET) transition between two dyes, Cyanine3 (Cy3) and Cyanine5 (Cy5), in the presence of bacteria. Additionally, the smart dressing is capable of treating bacterial infections through the release of antibiotics

triggered by near-infrared (NIR) light. However, pH may not always be indicative of infection. Other factors, such as inflammation or tissue damage, can also affect wound pH levels, leading to false positives and unnecessary treatments.

The delivery of oxygen to a wound can accelerate and improve wound healing. Oxygen is required for the production of reactive oxygen species (ROS), which are involved in clearing debris and fighting off infections during the inflammatory phase of wound healing. Additionally, oxygen is necessary for angiogenesis and collagen synthesis, which are essential steps in the formation of new blood vessels and tissues. Insufficient oxygen supply can lead to delayed or impaired wound healing, causing chronic wounds or non-healing ulcers. By providing a sufficient supply of oxygen to the wound site, an oxygen delivery device can enhance cellular processes, resulting in faster wound closure and reduced complications. Oxygen delivery devices may be especially beneficial for patients with underlying health conditions that impair their ability to transport oxygen to the wound site.

Ochoa *et al.* developed a low-cost alternative for continuous delivery and sensing of oxygen. The platform was made of an inexpensive, biocompatible, and flexible paper-based substrate that generates and measures oxygen in a wound region. The system takes advantage of recent developments in flexible microsystems and inkjet printing technology. The platform was able to increase oxygen concentration in a gel substrate by 13% (5 ppm) in 1 hour and was capable of sensing oxygen in a range of 5–26 ppm. On the other hand, Lo *et al.* developed a new type of wound dressing that uses microfluidic diffusion to deliver oxygen.<sup>247</sup> This bandage not only controls the amount of oxygen delivered but also creates a seal that conforms to the wound. When 100% oxygen is delivered, it enters the wound tissues and increases the oxygen levels at the site, thereby promoting healing.

Microfluidic platforms are utilized for delivering therapeutic agents such as drugs and growth factors directly to the wound site. As mentioned earlier, these platforms also help in studying cellular responses to mechanical and chemical stimuli under controlled conditions. The application of microfluidics in wound healing research has resulted in the creation of innovative techniques to facilitate wound closure and tissue regeneration.<sup>248</sup> This includes the targeted delivery of oxygen and nutrients to the wound area and the generation of gradients of signalling molecules to direct cell migration and differentiation.<sup>248–251</sup> Huang *et al.* developed a new method for creating fibres using microfluidic spinning technology that can carry two different types of cargo and release them when needed.<sup>252</sup> Fig. 8a provides an illustration of microfluidic spinning and collection of dual-cargo-loaded microfibers. This is achieved by combining biomaterials with hydrophobic and hydrophilic properties to form a bead-on-string microfibre structure. The team reported successful loading of bovine serum albumin (BSA) in the sodium alginate phase and ibuprofen in the polylactic acid (PLA) phase. The resulting

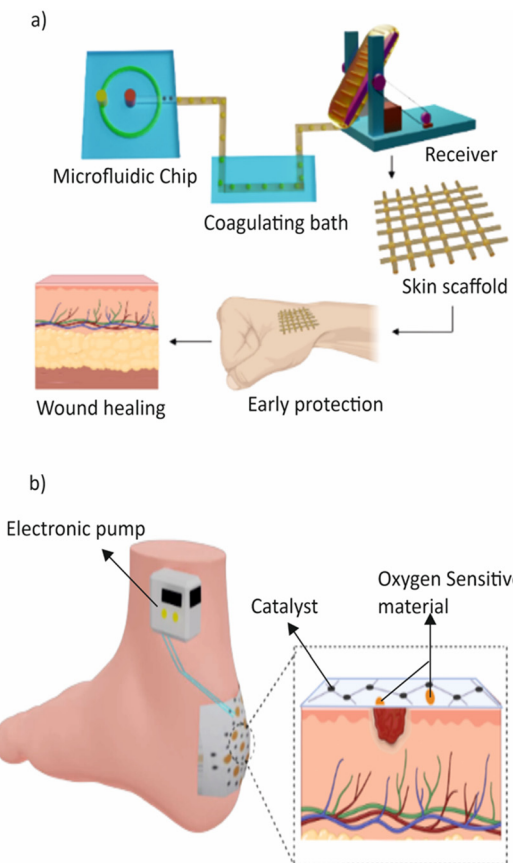


**Fig. 8** a) Illustration of microfluidic spinning and collection of dual-cargo-loaded microfibers. These biocompatible fibres are used for quick haemostasis and wound healing. b) Schematic representation of the oxygen sensing and delivery patch for foot ulcers and cross-sectional view of the smart patch and wound area.

fibres are biocompatible and can stop bleeding in live animals. When woven into a skin scaffold and loaded with antibacterial and anti-inflammatory agents, the fibres have the potential to promote faster wound healing. Fig. 8b shows a schematic representation of the oxygen sensing and delivery patch for foot ulcers along with a cross-sectional area of the wound.<sup>253</sup> While microfluidic devices and smart bandages offer several advantages in wound healing, they may still require the supervision of a medical expert.

**3.6.2. Challenges and outlook.** Smart bandages face several obstacles in wound healing, such as the high costs and intricate procedures involved in integrating sensors and electronics into the bandage material. Moreover, ensuring the dependable and precise collection of data and resolving potential concerns related to power supply and data transmission are also challenges that must be addressed. Furthermore, incorporating multiple functionalities like drug delivery and wound monitoring can increase the complexity and expenses of smart bandages. To ensure their safety and long-term use, materials used in the bandage need to be biocompatible. The complexity of the wound environment, which varies depending on the type and extent of the injury, presents another challenge that must be addressed by

designing microfluidic devices that can accommodate this variability and offer personalized treatment. While microfluidic devices have the potential to significantly enhance wound healing, they must be affordable and accessible to patients and healthcare providers to be widely adopted. And also, a customized approach may be needed for optimal healing. This is because the wound environment can be complex and variable.

#### 4. Smart wearable microfluidic devices

Following the introduction of digital hearing aids in the 1980s, wearables have undergone significant transformations, evolving in form and functionality.<sup>254</sup> One area that has seen substantial growth is the integration of microfluidics into healthcare wearables. However, the development of wearable microfluidic devices for commercialization faces challenges related to miniaturization, integration, and intelligence. Recent advancements in microfluidics have explored the fusion of artificial intelligence (AI) technologies, leading to the emergence of intelligent microfluidic devices.<sup>255</sup> Fig. 9a illustrates examples of typical advanced wearable devices.<sup>102</sup>

The healthcare industry has been benefitting from the rapid growth of cutting-edge technologies such as the Internet of Things (IoT),<sup>256</sup> artificial intelligence (AI),<sup>257</sup> and the Internet of Medical Things (IoMT).<sup>258</sup> These technologies, once confined to the realm of science fiction, have become a tangible reality, affecting various aspects of our lives. Their integration has expanded the capabilities and functionalities of wearable devices. AI and IoT offer robust high-dimensional data processing capabilities, particularly in disease diagnostics and fatigue monitoring, paving the way for personalized medicine and improved patient outcomes. AI enables real-time analysis and decision-making, while IoT and IoMT facilitate seamless data exchange and remote monitoring. The integration of IoT into microfluidic devices has gained momentum, driven by the rapid growth of automation and wireless networks. This advancement enables the creation of remotely controlled and monitored microfluidic devices, facilitating on-site analysis and monitoring.<sup>259,260</sup>

The increasing dependence on AI in the healthcare sector is evident in the projected growth of global artificial intelligence in the healthcare market, which is expected to reach USD 31.3 billion by 2025, with a remarkable CAGR of 41.5% (according to Grand View Research, Inc.).<sup>261</sup> This substantial growth reflects the expanding scope and potential of AI in improving healthcare outcomes and transforming the industry.

The following sections explore the recent developments in the integration of AI, IoT, IoMT and IoP in microfluidic wearable devices for on-site performance, address the challenges and limitations faced, and discuss potential future directions. By examining the convergence of these technologies, we can gain valuable insights into their impact

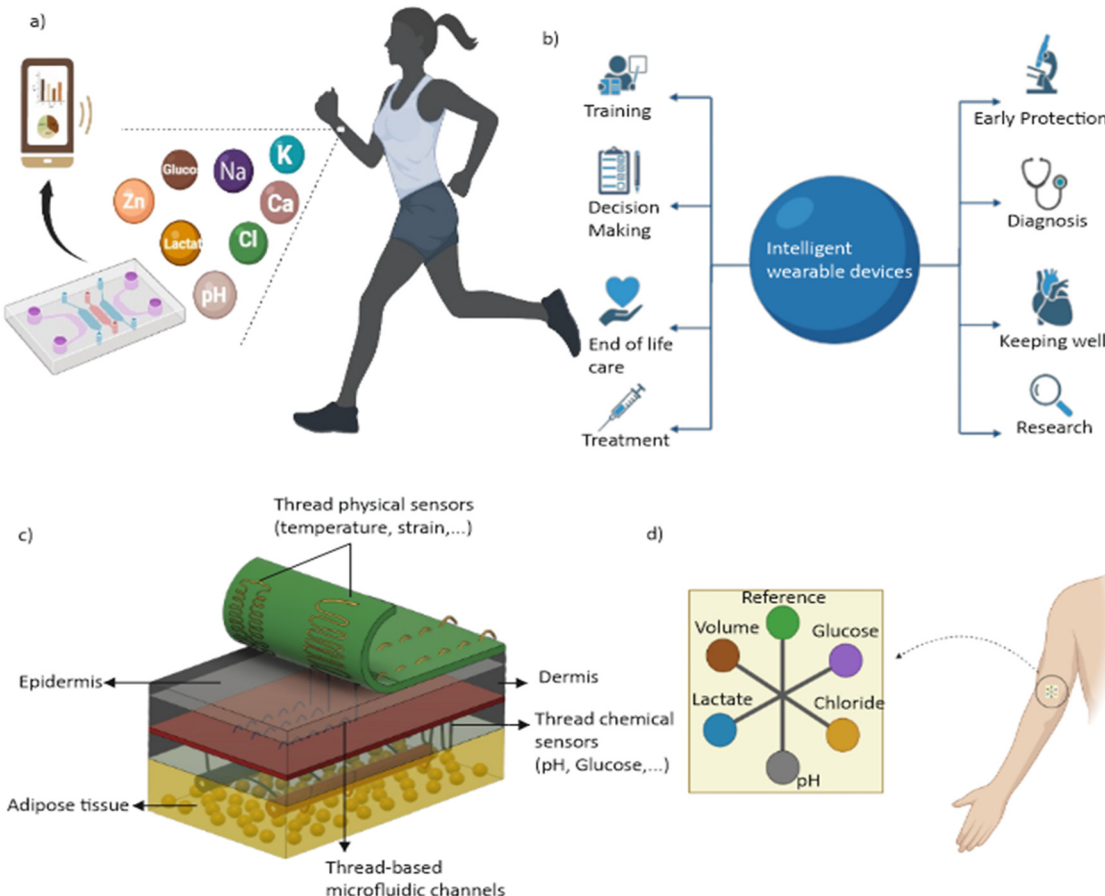


**Fig. 9** a) Conceptual diagram of an intelligent wearable microfluidic device. b) Representation of the advantages of intelligent wearable devices. c) Schematic representation of thread-based microfluidic networks that establish close connections with biological tissues in a three-dimensional manner. d) Illustration of an IoT-based microfluidic cellulose-based wearable patch.

on the development of intelligent, connected, and user-centric microfluidic-based wearable devices. For ease of reference, advantages of the intelligent wearable devices are illustrated in Fig. 9b.<sup>102</sup>

#### 4.1. Artificial intelligence and microfluidic wearable devices

Artificial intelligence (AI) is the simulation of human intelligence processes by computer systems. These processes include learning (the acquisition of information and rules for using the information), reasoning (using the rules to reach approximate or definite conclusions), and self-correction.<sup>262</sup> Artificial intelligence (AI) techniques, including machine learning and deep learning algorithms, have gained significant attention in recent years due to their ability to analyse complex data, recognize patterns, and make real-time decisions. In the context of microfluidics-based wearable devices, AI empowers these devices with intelligent data processing, predictive modelling, and adaptive control capabilities. By harnessing AI algorithms, these devices can extract valuable insights from the vast amount of data generated by microfluidic systems, leading to improved

diagnostics, personalized treatment strategies, and real-time monitoring of health conditions.<sup>255,263</sup>

AI in wearable microfluidic devices offers valuable applications in data analysis and decision-making. AI algorithms excel at extracting meaningful patterns and interpreting complex data, enabling precise diagnostics, continuous monitoring, and personalized treatment recommendations.<sup>264</sup> Furthermore, AI's predictive analytics capabilities enable early disease detection, prognosis assessment, and preventive interventions based on historical data. Intelligent control and automation represent another area where AI enhances wearable devices, driving significant advancements in healthcare.<sup>265</sup>

In microfluidic wearable devices, conventional control systems typically operate using fixed algorithms and predetermined rules.<sup>266</sup> These systems adhere to predefined instructions for tasks like drug release or parameter monitoring. While functional, they exhibit a lack of adaptability to dynamically changing conditions. In contrast, AI-based control systems introduce a transformative approach to microfluidic wearables. Rather than relying on static rules, these systems depend on machine learning algorithms to analyze real-time data.<sup>267</sup> This empowers them

to make decisions based on the current context, learning and adapting over time.<sup>268</sup>

AI-based control systems offer considerable advantages in the design of drug delivery devices, especially in the context of diabetes management. In comparison to conventional control systems that administer insulin at predetermined intervals, regardless of the wearer's immediate blood glucose levels, AI-based systems can dynamically adjust the insulin dosage based on real-time glucose monitoring.<sup>269</sup> However, AI-based systems present a more sophisticated and responsive approach.<sup>270</sup> These AI-driven systems can continuously monitor glucose levels, assimilate patterns over time, and dynamically adjust insulin dosages accordingly. This dynamic response ensures more effective blood sugar control, significantly reducing the risks associated with hypoglycemia or hyperglycemia. The benefits of AI-based control extend beyond adaptability, demonstrating notable strengths in personalization. These systems excel at tailoring responses based on individual user data, providing a level of customization that is challenging for conventional systems to achieve.

Moreover, the significance of AI-based control systems extends to critical tasks such as fluid mixing within microfluidic devices, where precise combinations of fluids are paramount.<sup>265</sup> Traditional systems may encounter challenges in adapting to variations in fluid properties, concentrations, or environmental factors. Conversely, AI-driven microfluidic systems excel at optimizing mixing ratios, ensuring the achievement of accurate and consistent results. Similarly, in the context of flow control, AI-based systems demonstrate a heightened level of sophistication and responsiveness.<sup>271,272</sup> These systems can dynamically regulate flow rates based on real-time data, adapting seamlessly to changes in fluid viscosity or external environmental conditions.<sup>273</sup> This heightened adaptability contributes to the overall efficiency and performance of microfluidic wearables, offering a level of precision that is particularly crucial in processes such as drug delivery or diagnostic procedures.<sup>270</sup> The dynamic adjustment of flow rates ensures that the microfluidic processes remain finely tuned, providing a more accurate and personalized experience within the wearable device.<sup>274</sup>

AI significantly contributes to personalized medicine as well by analysing patient-specific data, including genetic information, biomarker profiles, and physiological parameters. AI algorithms can develop tailored treatment plans.<sup>275</sup> These plans consider individual characteristics, allowing for personalized therapies, precise dosages, and targeted interventions, ultimately leading to improved healthcare outcomes. Furthermore, they have the potential to revolutionize disease monitoring and management. Through continuous monitoring and real-time feedback, these devices detect changes in biomarkers, track disease progression, and trigger timely interventions. This proactive approach to healthcare management reduces the risk of complications and empowers both patients and healthcare providers with actionable insights. Moreover, AI facilitates the fusion and integration of data within wearable devices.<sup>265</sup> These devices seamlessly integrate data from various sources, such as physiological measurements,

genetic data, and environmental factors. By combining these diverse data streams, AI algorithms uncover hidden relationships and provide a comprehensive understanding of an individual's health. This comprehensive understanding enables healthcare professionals to make more informed decisions.

The integration of artificial intelligence (AI) with point-of-care microfluidic devices has indeed seen notable progress.<sup>270</sup> However, the extension of this synergy to microfluidic wearable devices within the same domain faces certain limitations. Several factors contribute to the current absence of widespread AI-driven wearable microfluidic devices. The challenges lie in the complexity of merging AI algorithms with the miniaturized and portable nature of wearable microfluidic devices. While microfluidic devices at point-of-care settings benefit from integrated AI for improved diagnostics or treatment optimization, scaling down these capabilities for wearables introduces additional technical hurdles. In Table 3, various examples of microfluidic devices associated with AI-based control systems are likely presented. These could encompass devices designed for tasks such as flow control, mixing and particle manipulation. These devices leverage AI algorithms to process the data obtained from microfluidic components, allowing for more sophisticated and adaptive functionality.<sup>23</sup>

#### 4.2. Machine learning and deep learning in microfluidics

Machine Learning (ML) is an integral part of artificial intelligence and serves as its core. ML algorithms construct models using sample data, known as training data, enabling them to make predictions or decisions without explicit programming.<sup>276</sup> The fundamental elements of ML are data, algorithms (models), and computational power. ML particularly excels in tasks involving high-dimensional data, such as classification, regression, and clustering.<sup>277</sup> ML proves to be highly useful, as it learns from past computations and extracts patterns from extensive databases, resulting in reliable and consistent decision-making. The field of machine learning has seen remarkable progress in recent years, particularly in the context of wearable devices that collect high-dimensional data on users' health.<sup>278</sup> Machine learning algorithms are capable of processing these data to extract insights and make predictions about an individual's health.

Machine learning (ML) encompasses two primary approaches: supervised learning and unsupervised learning. Supervised learning involves training ML algorithms using labelled data, where each data point is accompanied by its corresponding target or outcome.<sup>279</sup> The algorithm learns to map input variables to the desired output based on labelled training data. With this knowledge, ML can then make predictions or decisions for new, unseen data. Supervised learning is highly useful for tasks like classification and regression, where the goal is to predict a specific outcome. The advantage of supervised learning is that it can provide accurate predictions and make well-informed decisions based

**Table 3** Microfluidic devices utilizing artificial intelligence for various biofluids

Device	Biofluid	Technique used	Advantages	Ref.
µTPAD and 3D µPAD for glucose analysis	Artificial urine	Artificial neural network (ANN trained on CMYK colour data)	1. High accuracy in classifying samples (94.4% for µTPAD, 91.2% for µPAD)	265
Rare hereditary hemolytic anemia (RHHA) study using microfluidics	Blood	Deep learning (DL)	1. Enables user-independent, automatic analysis with image analysis modules 2. Supports continuous monitoring using low-cost time-lapse microscopy (TLM) equipment	284
Microfluidic chip for T-cell and B-cell isolation and detection	Blood	Support Vector Machine (SVM) with Histogram of Oriented Gradients (HOG)	1. Efficient separation of T-cells and B-cells from sub-microliter blood samples 2. Utilizes SVM with HOG and colour distribution features for fast and robust cell detection 3. Achieves high accuracy (94% for detection, 96% with cross-validation) in distinguishing T-cells and B-cells	267
Enhanced immunoassay system	Serum	Convolutional neural network (CNN)	1. Simultaneous detection of six cytokines with high sensitivity 2. Short processing time 3. Rapid and accurate machine-learning-based image processing using CNN	287
Soft microfluidic patch	Sweat	Guided image capture and automated analysis	1. Real-time monitoring of sweat profiles 2. Personalized fluid intake recommendations 3. Usable in a broad range of fitness levels and conditions	273

on labelled training data. On the other hand, unsupervised learning deals with unlabelled data, meaning that the input data does not come with predefined outcomes. Instead, the algorithm aims to find patterns, structures, or relationships within the data on its own. It does so by grouping similar data points or identifying underlying patterns that may exist. Unsupervised learning is often employed in tasks such as clustering or anomaly detection. One of the key advantages of unsupervised learning is its ability to discover hidden insights and uncover previously unknown patterns within data, providing valuable insights for further analysis.<sup>280–282</sup>

Both supervised and unsupervised learning methods have their respective advantages and use cases in machine learning.<sup>282</sup> Supervised learning allows for accurate predictions and decision-making based on labelled data, which is particularly valuable in scenarios with known desired outcomes. Unsupervised learning, on the other hand, can uncover hidden patterns and relationships in unlabelled data, providing valuable insights and opportunities for further exploration.

Deep learning is a subfield of artificial intelligence (AI) that focuses on training artificial neural networks to learn and make predictions or decisions without explicit programming.<sup>283</sup> The process involves training deep neural networks with multiple layers to extract and understand complex patterns and representations from large datasets. In the context of microfluidic wearable devices, deep learning can be utilized for various tasks such as data analysis, decision-making, and control. The training process involves feeding the neural network with labelled or unlabelled data, depending on whether it's supervised or unsupervised learning.<sup>284</sup>

Deep neural networks find significant applications in medical diagnostics, where the pivotal role of supervised learning becomes evident.<sup>285</sup> In the context of wearable

devices, supervised learning is harnessed to train deep learning models using labelled datasets. These datasets comprise input samples such as physiological measurements and environmental factors, paired with corresponding output labels indicating specific health conditions or disease states. Through this process, the deep learning model learns to associate input data with their respective labels, enabling accurate predictions or classifications on new, unseen data.

A critical element in supervised deep learning is the definition and utilization of a loss function.<sup>286</sup> This function serves as a metric for the disparity between the model's predictions and the true labels in the dataset.<sup>286</sup> The minimization of this loss involves backpropagation, a technique where the computed loss is systematically propagated backwards through the neural network, influencing the model's parameters.<sup>287</sup> This iterative refinement allows the model to learn and enhance its performance over time. The ultimate objective is to update the model's parameters iteratively, improving its ability to make accurate predictions on unseen data.<sup>276</sup>

Microfluidic platforms, when coupled with deep learning algorithms, provide a versatile framework for simulating physiological conditions and studying various disorders. The application of deep learning in microfluidics allows for efficient data analysis and pattern recognition in dynamic biological systems. Comparative analyses of various deep learning architectures, including baseline convolutional neural networks (CNNs), SimpleNet, and CapsNet, reveal insights into their strengths and weaknesses.<sup>288</sup> Recurrent neural networks (RNNs), known for their sequential data processing capabilities, find application in microchip design for diagnostics.<sup>289</sup> Utilizing RNNs, particularly variants like long short-term memory (LSTM), allows for real-time processing of time-series data, showcasing the flexibility of deep learning in handling dynamic information.

On the other hand, unsupervised learning involves training the deep learning model using unlabelled data. Without explicit labels, the model focuses on discovering hidden patterns or structures within the data. Unsupervised learning is useful for tasks such as clustering, anomaly detection, and dimensionality reduction. In microfluidics, unsupervised learning can help to identify distinct groups or clusters of samples based on their characteristics or detect unusual patterns that may indicate abnormalities or outliers in the data.<sup>290,291</sup>

Both supervised and unsupervised learning methods have their advantages in wearable microfluidic devices. Supervised learning allows for targeted predictions or classifications based on known labels, which can be beneficial for specific diagnostic or monitoring applications. Unsupervised learning, on the other hand, provides a data-driven approach to uncovering patterns and relationships within complex microfluidic datasets, enabling researchers to gain insights and discover novel information without prior knowledge or assumptions.

Baker *et al.* present an updated wearable microfluidic sweat testing system for recreational athletes that includes a microfluidic patch and a smartphone app that can analyse sweat in real time using digital image processing algorithms (ML).<sup>292</sup> The microfluidic patch can accommodate a broad range of sweating rates, and the smartphone app can analyse the sweat under different lighting conditions and patch orientations. In another study, Ning *et al.* reported a rapid segmentation and sensitive analysis of CRP with a paper-based microfluidic device using machine learning.<sup>293</sup> The study involves the fabrication of multi-layer  $\mu$ PADs using the imprinting method for colorimetric detection of C-reactive protein (CRP). The detection-related performance of the  $\mu$ PADs is enhanced by utilizing a machine learning algorithm, specifically, the You Only Look Once (YOLO) model,<sup>294</sup> which is capable of identifying the reaction areas in the  $\mu$ PADs under different lighting conditions and shooting angles of scenes. The YOLO model was trained in the study and was able to quickly and accurately identify all reaction areas without error. The reaction areas were then characterized by classification algorithms to determine the risk level of CRP concentration. A microfluidic ultrafine particle dosimeter using an electrical detection method with a machine-learning-aided algorithm for real-time monitoring of particle density and size distribution was also reported. Mostafalu *et al.* developed thread-based microfluidic networks that establish close connections with biological tissues in a three-dimensional manner, Fig. 9c.<sup>295</sup> The research also involves the creation of a range of physical and chemical sensors, which are seamlessly integrated into these microfluidic networks. These sensors are fabricated using conductive threads infused with nanomaterials and are interconnected with electronic circuitry through flexible thread-based interconnects. This setup allows for the measurement and monitoring of physiochemical tissue properties, facilitating direct integration with tissues and

enabling the implementation of a thread-based diagnostic device (TDD) platform.<sup>295</sup> To showcase the capabilities of our integrated sensor suite, we conducted experiments using TDD platforms to measure parameters such as strain, gastric pH, and subcutaneous pH both *in vitro* and *in vivo*.

While the field of wearable devices incorporating microfluidics and artificial intelligence holds immense promise, the limited prevalence of such devices prompts a closer examination of the challenges impeding their widespread adoption. Within the complex landscape of AI and data science, a series of nuanced challenges must be navigated before these innovative devices can proliferate.<sup>270</sup> One pivotal challenge lies in ensuring the generalizability of the AI models across diverse user populations. The ability of these models to adapt and perform effectively across various demographic and physiological characteristics is essential for their practical application.<sup>283</sup> Achieving this requires a thorough understanding of the complexities associated with different user contexts and the development of robust algorithms that can accommodate these variations.

Model complexity considerations represent another significant hurdle. Striking the right balance in model complexity is crucial to prevent issues such as overfitting or underfitting.<sup>263</sup> The intricacies of microfluidic data and the diverse nature of physiological measurements necessitate AI models that are sophisticated enough to capture relevant patterns yet not overly complex to hinder practical deployment. Ethical considerations add an additional layer of complexity.<sup>296,297</sup> The deployment of AI in wearable devices raises concerns related to data privacy, bias detection, and transparency in decision-making processes. Safeguarding user data, ensuring fairness in algorithmic outcomes, and maintaining transparency are paramount for responsible AI deployment in healthcare.

#### 4.3. Internet of Things and wearable microfluidic devices

The Internet of Things (IoT) is a network of physical devices, objects, and appliances equipped with sensors, software, and connectivity.<sup>298</sup> The IoT enables them to collect and exchange data over the internet, creating a seamless connection between the physical and digital worlds. In IoT, devices use sensors to gather data about their surroundings or interactions. These data include temperature, motion, and biometrics.<sup>299</sup> The devices process the data using internal processors, often in real time. IoT devices connect to the internet, allowing them to transmit data to cloud platforms or other devices. Communication occurs through protocols such as Wi-Fi, Bluetooth, or specialized IoT protocols. Advanced analytics and algorithms analyse data, generating valuable insights, detecting patterns, and triggering automated actions. Security is vital in IoT to protect data integrity and privacy.<sup>300</sup> Encryption, authentication, and access control mechanisms ensure that data are secured. The IoT has diverse applications, including smart homes,

industrial automation, agriculture, transportation systems, and healthcare monitoring.

The integration of IoT technology with microfluidic wearable devices is transforming the healthcare industry.<sup>301</sup> This combination of microfluidics and IoT connectivity brings new possibilities for diagnostics, monitoring, and personalized medicine. By connecting to the internet, microfluidic wearables can transmit real-time data, enabling remote monitoring of a patient's health.<sup>11</sup> Equipped with sensors, these wearables capture vital health parameters like biomarkers or fluid flow rates. The data are wirelessly sent to healthcare providers or cloud-based platforms for in-depth analysis using advanced analytics.

Real-time monitoring becomes a reality as healthcare professionals receive continuous updates on patients' conditions. Immediate alerts can be triggered for critical events or abnormal readings, facilitating timely interventions that can potentially save lives.<sup>302</sup> Remote monitoring is particularly beneficial for individuals with chronic conditions or those in remote areas.

The integration of IoT also brings data-driven insights and personalized healthcare. Advanced analytics algorithms process the collected data, identifying trends, patterns, and potential health issues.<sup>303</sup> This information empowers healthcare providers to make accurate diagnoses, create personalized treatment plans, and deliver proactive care. Patients can actively engage in their healthcare by accessing health data through mobile applications, setting goals, and receiving tailored recommendations.<sup>304</sup>

Additionally, the integration of microfluidic wearables with IoT offers scalability and interoperability.<sup>305</sup> These devices can be easily deployed across various healthcare settings, seamlessly integrating with existing systems, electronic health records, and other medical devices. The smooth exchange of data ensures a comprehensive understanding of a patient's health history and enables collaboration among healthcare professionals.<sup>306</sup>

Despite the numerous advantages and benefits of integrating IoT with microfluidic wearable devices, the availability of IoT-based microfluidic wearables is currently limited. However, Ardalan *et al.* have made significant progress in this area. The team developed a cellulose-based wearable patch, combined with a smartphone-based fluorescence imaging module and a custom smartphone app. This system allows for non-invasive and *in situ* multi-sensing of sweat biomarkers such as glucose, lactate, pH, chloride, and volume.<sup>307</sup> Fig. 9d shows the schematic illustration of the device. Their smart wearable sweat patch (SWSP) sensor consists of highly fluorescent sensing probes embedded in paper substrates, along with microfluidic channels made of cotton threads. These channels effectively collect sweat from the skin surface and transport it to the paper-based sensing probes. To capture digital images of the sensors, an imaging module was fabricated using a 3D printer and equipped with UV-LED lamps and an optical filter. These images are captured *via* a smartphone, which also features a specially

designed app with a detection algorithm to quantify the concentration of the biomarkers. Furthermore, the researchers proposed an IoT-based model for their SWSP sensor, envisioning its potential applications in the future. Field studies involving human subjects were conducted to assess the feasibility of the developed SWSP sensor for analysing sweat biomarkers.

In addition to wearability, integrated Internet of Things (IoT) will enhance the functionality of microfluidic devices. For instance, Yuan *et al.* discussed the design, fabrication, and implementation of an IoT-based electrochemical microfluidic system, utilizing 3D printing technology, for detecting free calcium concentration.<sup>308</sup> This system is capable of accurately measuring free calcium solutions within the desired concentration range of 0 to 40  $\mu\text{M}$  and transmitting signals to the cloud for data sharing. Consequently, this system offers a precise and real-time monitoring solution for various biomedical samples.

#### 4.4. Other smart technologies

Alongside artificial intelligence and the Internet of Things, there are other technologies with the potential to revolutionize healthcare when integrated with microfluidic wearable devices. Two notable examples include the Internet of Medical Things (IoMT) and the Internet of People (IoP). These technologies hold immense capabilities for transforming healthcare by connecting medical devices and individuals, respectively.

The Internet of Medical Things (IoMT) facilitates the connection and communication between medical devices, sensors, and systems through the internet.<sup>258</sup> When combined with microfluidic wearable devices, the IoMT enables seamless real-time monitoring and data collection. This integration allows healthcare professionals to continuously track vital signs, analyse biofluids, and monitor various health parameters remotely. By harnessing the power of IoMT, medical practitioners gain access to accurate and up-to-date information, leading to enhanced diagnostics, personalized treatments, and proactive preventive care.<sup>309</sup> On the other hand, the Internet of People (IoP) focuses on interconnectivity between individuals and their surrounding devices. When merged with microfluidic wearable devices, the IoP empowers individuals to actively participate in managing their health.<sup>310</sup> Through wearable devices integrated with IoP, users can effortlessly track their health metrics, receive personalized health recommendations, and even share their data with healthcare providers.<sup>311</sup> This collaborative approach promotes proactive healthcare management, early detection of potential health issues, and seamless communication between patients and medical professionals.

#### 4.5. Challenges and outlook

The integration of microfluidic technology with advanced technologies such as AI, IoT, IoMT, and IoP in wearable

devices is an emerging and complex field that faces several challenges.<sup>312</sup> As a result, the number of commercially available microfluidic wearable devices integrated with these technologies is currently limited. One key challenge is the complexity of integration. Microfluidic devices are intricate systems that require precise fabrication and assembly of fluidic channels, sensors, and actuators. Incorporating AI, IoT, IoMT, and IoP into these devices adds a layer of complexity in terms of hardware, software, and connectivity requirements.<sup>11</sup> Developing reliable and robust integration methods necessitates extensive research and development efforts.

Moreover, there are significant technological hurdles to overcome. One significant challenge revolves around power consumption, as these devices must operate efficiently within limited power constraints to ensure prolonged usability without frequent recharging. Achieving a balance between computational power and energy efficiency is imperative for the success of such wearable devices. Another crucial aspect is the miniaturization and seamless integration of AI components into the microfluidic platform. Given the restricted physical space available, designing and incorporating compact AI hardware without compromising overall device performance is a non-trivial task.<sup>287</sup> The quality and quantity of data present additional hurdles. Gathering representative data from microfluidic experiments, while maintaining accuracy and relevance, is vital for training robust AI models. Optimization of algorithms specific to microfluidic data characteristics is also essential for effective model performance. Interdisciplinary collaboration is fundamental, as the development of AI-integrated microfluidic wearable devices requires expertise in microfluidics, AI, materials science, and other fields.<sup>264</sup> Bridging the interdisciplinary gap is crucial for a comprehensive understanding and successful device development.

Security and privacy concerns must not be overlooked. The integration of various technologies, including ML, IoT, and AI, into microfluidic devices introduces a spectrum of ethical considerations and social security challenges. These multifaceted issues require careful examination to ensure responsible and equitable deployment.<sup>296</sup> From an ethical standpoint, obtaining informed consent for data collection and addressing concerns related to data ownership and control are paramount.<sup>313</sup> Transparency in ML algorithms, regardless of whether they involve AI, is crucial to build trust and mitigate biases that may affect medical diagnostics. Privacy standards must be rigorously upheld to protect sensitive health information collected by IoT-enabled microfluidic devices. Security measures become even more critical when considering the interconnected nature of IoT. Safeguarding against cyber threats and unauthorized access to data and devices is essential to maintain the integrity and confidentiality of information.<sup>314</sup> Ensuring fairness in ML algorithms and preventing discrimination are an ethical imperative, especially when these technologies are applied in healthcare settings.

Additionally, regulatory and standard considerations play a vital role in the development and commercialization of

medical devices, including microfluidic wearables. Adhering to regulatory guidelines and obtaining necessary certifications can be a time-consuming and resource-intensive process, further delaying the introduction of integrated microfluidic wearable devices to the market. Moreover, future research should focus on investigating potential biases that may arise from measurement sources, particularly considering the variability in fluid compositions among diverse user populations. Understanding how different demographic and physiological factors can introduce bias in microfluidic measurements is crucial for developing robust and unbiased AI algorithms. This exploration is essential not only for enhancing the accuracy and reliability of AI-integrated microfluidic devices but also for ensuring equitable and unbiased healthcare solutions across various user demographics.

Despite these challenges, ongoing research and technological advancements continue to pave the way for the future development and commercialization of microfluidic wearable devices integrated with AI, IoT, IoMT, and IoP. As the field progresses, we can anticipate increased innovation, improved integration methods, and a broader range of microfluidic wearable devices that leverage these advanced technologies to enhance healthcare outcomes.

## 5. Conclusion

Microfluidics has emerged as a truly exciting and promising technology that holds great potential in the field of healthcare. Its unique ability to handle small sample volumes, perform rapid reactions, and achieve high sensitivity and throughput data has opened up a world of possibilities across diverse fields.<sup>11</sup>

The integration of microfluidics with advanced technologies like microelectronics, biosensors, soft materials, and artificial intelligence (AI) has led to the development of wearable microfluidics, a groundbreaking innovation with immense promise in the realm of medical diagnosis and personalized healthcare.<sup>254</sup> By combining the power of microfluidics with AI-driven data analytics and machine learning (ML), we can now envision wearable devices that provide real-time diagnostic information to patients. This remarkable combination allows for high-throughput analysis of small sample volumes and advanced data processing, unlocking potential breakthroughs in cell sorting, biomolecular analysis, and many more.

Looking towards the future, the potential of microfluidics lies in the region of intelligent systems. As we venture into an interconnected era where energy, electronics, communication, computers, and sensors converge, intelligent microfluidic systems will serve as powerful platforms for biomedical analysis. Moreover, the integration of microfluidics with other cutting-edge technologies such as the Internet of Things (IoT), Internet of Medical Things (IoMT), and Internet of People (IoP) amplifies the transformative capabilities of these wearable devices.

While the integration of these advanced technologies with wearable microfluidic devices brings tremendous promise, it is crucial to acknowledge the challenges that lie ahead. Technical complexities, standardization efforts, regulatory considerations, and user acceptance all demand further attention and refinement to ensure successful implementation.

Looking ahead, we anticipate that intelligent microfluidics will play an increasingly crucial role in both research and industry. These integrated wearable devices offer the potential to revolutionize healthcare and personalized medicine, empowering individuals with accurate biofluid analysis, remote monitoring capabilities, and personalized treatments. As research progresses and we continue to push the boundaries, we can expect the development of even more sophisticated and interconnected wearable microfluidic devices. Ultimately, this progress will pave the way for improved healthcare outcomes, preventive care, and a better quality of life for individuals around the globe.

In summary, the integration of microfluidics with wearable technology and intelligence technologies such as AI, IoT, IoMT, and IoP represents an exciting frontier in healthcare and personalized medicine. By combining the elegance of microfluidics with these advanced technologies, we embark on a journey of innovation and transformation. The possibilities are vast, and as we advance, we move closer to a future where microfluidic wearable devices bring about tangible improvements in healthcare, revolutionizing the way we diagnose, monitor, and treat medical conditions.

## Conflicts of interest

The authors declare no conflicts of interest.

## Acknowledgements

Kamalalayam Rajan Sreejith acknowledges the financial support provided by Griffith University through the Griffith University Postdoctoral Fellowship. Nam-Trung Nguyen acknowledges funding support from the Australian Research Council through the Australian Laureate Fellowship FL230100023.

## References

- 1 J. Heikenfeld, A. Jajack, J. Rogers, P. Gutruf, L. Tian, T. Pan, R. Li, M. Khine, J. Kim, J. Wang and J. Kim, *Lab Chip*, 2018, **18**, 217–248.
- 2 G. Aroganam, N. Manivannan and D. Harrison, *Sensors*, 2019, **19**, 1983.
- 3 Fitbit Official Site for Activity Trackers and More, <https://www.fitbit.com/global/in/home>, (accessed 18 April 2023).
- 4 Monitor your heart rate with Apple Watch, <https://support.apple.com/en-in/HT204666>, (accessed 18 April 2023).
- 5 G. L. or its subsidiaries, Fitness Tracker|Wearables, <https://www.garmin.co.in/products/wearables/>, (accessed 18 April 2023).
- 6 B. J. van Enter and E. von Hauff, *Chem. Commun.*, 2018, **54**, 5032–5045.
- 7 P. Kamga, R. Mostafa and S. Zafar, *Curr. Emerg. Hosp. Med. Rep.*, 2022, **10**, 67–72.
- 8 A. Channa, N. Popescu, J. Skibinska and R. Burget, *Sensors*, 2021, **21**, 5787.
- 9 Gartner Forecasts Global Spending on Wearable Devices to Total \$81.5 Billion in 2021, <https://www.gartner.com/en/newsroom/press-releases/2021-01-11-gartner-forecasts-global-spending-on-wearable-devices-to-total-81-5-billion-in-2021>, (accessed 2 April 2023).
- 10 C. Wu, P. Jiang, W. Li, H. Guo, J. Wang, J. Chen, M. R. Prausnitz and Z. L. Wang, *Adv. Funct. Mater.*, 2020, **30**, 1907378.
- 11 J. R. Mejia-Salazar, K. Rodrigues Cruz, E. M. Materón Vásques and O. Novais de Oliveira Jr, *Sensors*, 2020, **20**, 1951.
- 12 Y. Xing, L. Zhao, Z. Cheng, C. Lv, F. Yu and F. Yu, *ACS Appl. Bio Mater.*, 2021, **4**, 2160–2191.
- 13 F. Gao, C. Liu, L. Zhang, T. Liu, Z. Wang, Z. Song, H. Cai, Z. Fang, J. Chen, J. Wang, M. Han, J. Wang, K. Lin, R. Wang, M. Li, Q. Mei, X. Ma, S. Liang, G. Gou and N. Xue, *Microsyst. Nanoeng.*, 2023, **9**, 1.
- 14 J. Choi, A. J. Bandodkar, J. T. Reeder, T. R. Ray, A. Turnquist, S. B. Kim, N. Nyberg, A. Hourlier-Fargette, J. B. Model, A. J. Aranyosi, S. Xu, R. Ghaffari and J. A. Rogers, *ACS Sens.*, 2019, **4**, 379–388.
- 15 S. Damiati, U. Kompella, S. Damiati and R. Kodzius, *Genes*, 2018, **9**, 103.
- 16 T. Sun, J. Hui, L. Zhou, B. Lin, H. Sun, Y. Bai, J. Zhao and H. Mao, *Sens. Actuators, B*, 2022, **368**, 132184.
- 17 J.-D. Huang, J. Wang, E. Ramsey, G. Leavey, T. J. A. Chico and J. Condell, *Sensors*, 2022, **22**, 8002.
- 18 B. R. Schatz, *NPJ Digit. Med.*, 2018, **1**, 20174.
- 19 C. Y. Jin, *IOP Conf. Ser.: Mater. Sci. Eng.*, 2019, **688**, 044072.
- 20 S. A. Amyx+McKinsey, Wearing Your Intelligence, <https://www.wired.com/insights/2014/12/wearing-your-intelligence/>, (accessed 18 April 2023).
- 21 F. John Dian, R. Vahidnia and A. Rahmati, *IEEE Access*, 2020, **8**, 69200–69211.
- 22 S. Radhakrishnan, M. Mathew and C. S. Rout, *Mater. Adv.*, 2022, **3**, 1874–1904.
- 23 H.-F. Tsai, S. Podder and P.-Y. Chen, *Micromachines*, 2023, **14**, 826.
- 24 S. Shrivastava, T. Q. Trung and N.-E. Lee, *Chem. Soc. Rev.*, 2020, **49**, 1812–1866.
- 25 Anushka, A. Bandopadhyay and P. K. Das, *Eur. Phys. J.: Spec. Top.*, 2023, **232**(6), 781–815.
- 26 Y. Yang, E. Noviana, M. P. Nguyen, B. J. Geiss, D. S. Dandy and C. S. Henry, *Anal. Chem.*, 2017, **89**, 71–91.
- 27 X. Zhang, L. Li and C. Luo, *Lab Chip*, 2016, **16**, 1757–1776.
- 28 H. H. Caicedo and S. T. Brady, *Trends Biotechnol.*, 2016, **34**, 1–3.
- 29 W. Yang, W. Han, H. Gao, L. Zhang, S. Wang, L. Xing, Y. Zhang and X. Xue, *Nanoscale*, 2018, **10**, 2099–2107.
- 30 S. R. Corrie, J. W. Coffey, J. Islam, K. A. Markey and M. A. F. Kendall, *Analyst*, 2015, **140**, 4350–4364.

31 S. A. N. Gowers, V. F. Curto, C. A. Seneci, C. Wang, S. Anastasova, P. Vadgama, G.-Z. Yang and M. G. Boutelle, *Anal. Chem.*, 2015, **87**, 7763–7770.

32 M. Chung, G. Fortunato and N. Radacs, *J. R. Soc., Interface*, 2019, **16**, 20190217.

33 J. C. Jokerst, J. M. Emory and C. S. Henry, *Analyst*, 2012, **137**, 24–34.

34 S. He, N. Joseph, S. Feng, M. Jellicoe and C. L. Raston, *Food Funct.*, 2020, **11**, 5726–5737.

35 H. Tabasum, N. Gill, R. Mishra and S. Lone, *RSC Adv.*, 2022, **12**, 8691–8707.

36 S. Scott and Z. Ali, *Micromachines*, 2021, **12**, 319.

37 A. Couto and T. Dong, in *2017 39th Annual International Conference of the IEEE Engineering in Medicine and Biology Society (EMBC)*, IEEE, Seogwipo, 2017, pp. 181–184.

38 K. T. L. Trinh and N. Y. Lee, *Biosensors*, 2022, **12**, 72.

39 M. Sonker, V. Sahore and A. T. Woolley, *Anal. Chim. Acta*, 2017, **986**, 1–11.

40 G. Rong, Y. Zheng and M. Sawan, *Sensors*, 2021, **21**, 3806.

41 M. Gao, P. Wang, L. Jiang, B. Wang, Y. Yao, S. Liu, D. Chu, W. Cheng and Y. Lu, *Energy Environ. Sci.*, 2021, **14**, 2114–2157.

42 A. Shakeri, S. Khan and T. F. Didar, *Lab Chip*, 2021, **21**, 3053–3075.

43 K. Ganeson, A. H. Alias, V. Murugaiyah, A.-A. A. Amirul, S. Ramakrishna and S. Vigneswari, *Pharmaceutics*, 2023, **15**, 744.

44 I. Miranda, A. Souza, P. Sousa, J. Ribeiro, E. M. S. Castanheira, R. Lima and G. Minas, *JFB*, 2021, **13**, 2.

45 J. C. Love, J. R. Anderson and G. M. Whitesides, *MRS Bull.*, 2001, **26**, 523–528.

46 V. N. Goral, Y.-C. Hsieh, O. N. Petzold, R. A. Faris and P. K. Yuen, *J. Micromech. Microeng.*, 2011, **21**, 017002.

47 U. N. Lee, X. Su, D. J. Guckenberger, A. M. Dostie, T. Zhang, E. Berthier and A. B. Theberge, *Lab Chip*, 2018, **18**, 496–504.

48 R. S. Kane, A. D. Stroock, N. Li Jeon, D. E. Ingber and G. M. Whitesides, in *Optical Biosensors*, Elsevier, 2002, pp. 571–595.

49 K. Raj M and S. Chakraborty, *J. Appl. Polym. Sci.*, 2020, **137**, 48958.

50 A. M. Pentecost and R. S. Martin, *Anal. Methods*, 2015, **7**, 2968–2976.

51 T. Hamada, S. Hasegawa, H. Fukasawa, S. Sawada, H. Koshikawa, A. Miyashita and Y. Maekawa, *J. Mater. Chem. A*, 2015, **3**, 20983–20991.

52 L. Yang, Z. Zhang and X. Wang, *Micromachines*, 2022, **13**, 552.

53 D. Voicu, G. Lestari, Y. Wang, M. DeBono, M. Seo, S. Cho and E. Kumacheva, *RSC Adv.*, 2017, **7**, 2884–2889.

54 W. Zhang, S. Lin, C. Wang, J. Hu, C. Li, Z. Zhuang, Y. Zhou, R. A. Mathies and C. J. Yang, *Lab Chip*, 2009, **9**, 3088.

55 N. Keller, T. M. Nargang, M. Runck, F. Kotz, A. Striegel, K. Sachsenheimer, D. Klemm, K. Länge, M. Worgull, C. Richter, D. Helmer and B. E. Rapp, *Lab Chip*, 2016, **16**, 1561–1564.

56 D. Ogończyk, J. Węgrzyn, P. Jankowski, B. Dąbrowski and P. Garstecki, *Lab Chip*, 2010, **10**, 1324.

57 Polyetherimide (PEI) Polymer, <https://omnexus.specialchem.com/selection-guide/polyetherimide-pei-high-heat-plastic>, (accessed 19 April 2023).

58 L. A. Damiati, M. El-Yaagoubi, S. A. Damiati, R. Kodzius, F. Sefat and S. Damiati, *Polymer*, 2022, **14**, 5132.

59 M. Figurova, D. Pudis, P. Gaso and I. Cimrak, in *2016 ELEKTRO*, IEEE, Strbske Pleso, High Tatras, Slovakia, 2016, pp. 608–611.

60 G. Comina, A. Suska and D. Filippini, *Lab Chip*, 2014, **14**, 424–430.

61 I. Hoek, F. Tho and W. M. Arnold, *Lab Chip*, 2010, **10**, 2283.

62 Y. H. Ko, S. H. Lee, J. W. Leem and J. S. Yu, *RSC Adv.*, 2014, **4**, 10216.

63 M. P. Wolf, G. B. Salieb-Beugelaar and P. Hunziker, *Prog. Polym. Sci.*, 2018, **83**, 97–134.

64 B. Heo, M. Fiola, J. H. Yang and A. Koh, *Colloid Interface Sci. Commun.*, 2020, **38**, 100301.

65 M. W. Toepke and D. J. Beebe, *Lab Chip*, 2006, **6**, 1484.

66 E. Team, *Elveflow*.

67 A. K. Yetisen, M. S. Akram and C. R. Lowe, *Lab Chip*, 2013, **13**, 2210.

68 Z. Ye, Y. Yuan, S. Zhan, W. Liu, L. Fang and T. Li, *Analyst*, 2023, **148**, 1175–1188.

69 Z. Yao, P. Coatsworth, X. Shi, J. Zhi, L. Hu, R. Yan, F. Güder and H.-D. Yu, *Sens. Diagn.*, 2022, **1**, 312–342.

70 S. G. Yedire, H. Khan, T. AbdelFatah, R. Siavash Moakhar and S. Mahshid, *Sens. Diagn.*, 2023, **2**, 763–780.

71 W. Dungchai, O. Chailapakul and C. S. Henry, *Anal. Chem.*, 2009, **81**, 5821–5826.

72 B. Hu, J. Li, L. Mou, Y. Liu, J. Deng, W. Qian, J. Sun, R. Cha and X. Jiang, *Lab Chip*, 2017, **17**, 2225–2234.

73 E. Carrilho, A. W. Martinez and G. M. Whitesides, *Anal. Chem.*, 2009, **81**, 7091–7095.

74 H. Shibata, Y. Hiruta and D. Citterio, *Analyst*, 2019, **144**, 1178–1186.

75 L. Yu and Z. Z. Shi, *Lab Chip*, 2015, **15**, 1642–1645.

76 J. Olkkonen, K. Lehtinen and T. Erho, *Anal. Chem.*, 2010, **82**, 10246–10250.

77 X. Li, J. Tian, T. Nguyen and W. Shen, *Anal. Chem.*, 2008, **80**, 9131–9134.

78 G. Chitnis, Z. Ding, C.-L. Chang, C. A. Savran and B. Ziaie, *Lab Chip*, 2011, **11**, 1161.

79 L. Zhang, W. Wang, X.-J. Ju, R. Xie, Z. Liu and L.-Y. Chu, *RSC Adv.*, 2015, **5**, 5638–5646.

80 Y. Sameenoi, P. N. Nongkai, S. Nouanthatvong, C. S. Henry and D. Nacapricha, *Analyst*, 2014, **139**, 6580–6588.

81 U. Mogera, H. Guo, M. Namkoong, M. S. Rahman, T. Nguyen and L. Tian, *Sci. Adv.*, 2022, **8**, eabn1736.

82 T. Abbasiasl, F. Mirlou, E. Istif, H. Ceylan Koydemir and L. Beker, *Sens. Diagn.*, 2022, **1**, 775–786.

83 S. Nishat, A. T. Jafry, A. W. Martinez and F. R. Awan, *Sens. Actuators, B*, 2021, **336**, 129681.

84 E. Noviana, T. Ozer, C. S. Carrell, J. S. Link, C. McMahon, I. Jang and C. S. Henry, *Chem. Rev.*, 2021, **121**, 11835–11885.

85 S. Mdanda, P. Ubanako, P. P. D. Kondiah, P. Kumar and Y. E. Choonara, *Polymer*, 2021, **13**, 2405.

86 K. Ita, *Pharmaceutics*, 2015, **7**, 90–105.

87 R. Maia, V. Carvalho, R. Lima, G. Minas and R. O. Rodrigues, *Pharmaceutics*, 2023, **15**, 792.

88 J. H. Jung and S. G. Jin, *J. Pharm. Invest.*, 2021, **51**, 503–517.

89 T. Waghule, G. Singhvi, S. K. Dubey, M. M. Pandey, G. Gupta, M. Singh and K. Dua, *Biomed. Pharmacother.*, 2019, **109**, 1249–1258.

90 P. M. Wang, M. Cornwell, J. Hill and M. R. Prausnitz, *J. Invest. Dermatol.*, 2006, **126**, 1080–1087.

91 H.-R. Jeong, H. Jun, H.-R. Cha, J. Lee and J.-H. Park, *Micromachines*, 2020, **11**, 710.

92 Y. Ye, J. Yu, D. Wen, A. R. Kahkoska and Z. Gu, *Adv. Drug Delivery Rev.*, 2018, **127**, 106–118.

93 H. Kang, Z. Zuo, R. Lin, M. Yao, Y. Han and J. Han, *Drug Delivery*, 2022, **29**, 3087–3110.

94 A. Sionkowska, M. Gadomska, K. Musiał and J. Piątek, *Molecules*, 2020, **25**, 4035.

95 M. A. Luzuriaga, D. R. Berry, J. C. Reagan, R. A. Smaldone and J. J. Gassensmith, *Lab Chip*, 2018, **18**, 1223–1230.

96 Y. Su, S. M. Andрабی, S. M. S. Shahriar, S. L. Wong, G. Wang and J. Xie, *J. Controlled Release*, 2023, **356**, 131–141.

97 A. H. Sabri, Y. Kim, M. Marlow, D. J. Scurr, J. Segal, A. K. Banga, L. Kagan and J. B. Lee, *Adv. Drug Delivery Rev.*, 2020, **153**, 195–215.

98 Z. Zhao, Y. Chen and Y. Shi, *RSC Adv.*, 2020, **10**, 14040–14049.

99 J. Zhao, H. Guo, J. Li, A. J. Bandodkar and J. A. Rogers, *Trends Chem.*, 2019, **1**, 559–571.

100 N. Kashaninejad and N.-T. Nguyen, *Lab Chip*, 2023, **23**, 913–937.

101 J. Heikenfeld, A. Jajack, B. Feldman, S. W. Granger, S. Gaitonde, G. Begtrup and B. A. Katchman, *Nat. Biotechnol.*, 2019, **37**, 407–419.

102 Scientific Image and Illustration Software|BioRender, <https://www.biorender.com/>, (accessed 25 July 2023).

103 S. Solanki, C. M. Pandey, R. K. Gupta and B. D. Malhotra, *Biotechnol. J.*, 2020, **15**, 1900279.

104 L. B. Baker, *Temperature*, 2019, **6**, 211–259.

105 Y. Liu, T. Liu and D. Jiang, *Curr. Res. Biotechnol.*, 2023, **6**, 100143.

106 D. A. Kidwell, J. C. Holland and S. Athanasielis, *J. Chromatogr. B: Biomed. Sci. Appl.*, 1998, **713**, 111–135.

107 K. Van Hoovels, X. Xuan, M. Cuartero, M. Gijssel, M. Swarén and G. A. Crespo, *ACS Sens.*, 2021, **6**, 3496–3508.

108 Z. Sonner, E. Wilder, J. Heikenfeld, G. Kasting, F. Beyette, D. Swaile, F. Sherman, J. Joyce, J. Hagen, N. Kelley-Loughnane and R. Naik, *Biomicrofluidics*, 2015, **9**, 031301.

109 H. Tabasum, N. Gill, R. Mishra and S. Lone, *RSC Adv.*, 2022, **12**, 8691–8707.

110 T.-T. Luo, Z.-H. Sun, C.-X. Li, J.-L. Feng, Z.-X. Xiao and W.-D. Li, *J. Physiol. Sci.*, 2021, **71**, 26.

111 B. Schazmann, D. Morris, C. Slater, S. Beirne, C. Fay, R. Reuveny, N. Moyna and D. Diamond, *Anal. Methods*, 2010, **2**, 342.

112 H. Yoon, X. Xuan, S. Jeong and J. Y. Park, *Biosens. Bioelectron.*, 2018, **117**, 267–275.

113 H. Y. Nyein, W. Gao, Z. Shahpar, S. Emaminejad, S. Challa, K. Chen, H. M. Fahad, L. C. Tai, H. Ota, R. W. Davis and A. Javey, *ACS Nano*, 2016, **10**(7), 7216–7224.

114 Y. Zhang, H. Guo, S. B. Kim, Y. Wu, D. Ostojich, S. H. Park, X. Wang, Z. Weng, R. Li, A. J. Bandodkar, Y. Sekine, J. Choi, S. Xu, S. Quaggin, R. Ghaffari and J. A. Rogers, *Lab Chip*, 2019, **19**, 1545–1555.

115 L. B. Baker, M. S. Seib, K. A. Barnes, S. D. Brown, M. A. King, P. J. D. De Chavez, S. Qu, J. Archer, A. S. Wolfe, J. R. Stofan, J. M. Carter, D. E. Wright, J. Wallace, D. S. Yang, S. Liu, J. Anderson, T. Fort, W. Li, J. A. Wright, S. P. Lee, J. B. Model, J. A. Rogers, A. J. Aranyosi and R. Ghaffari, *Adv. Mater. Technol.*, 2022, **7**, 2200249.

116 P. Pirovano, M. Dorrian, A. Shinde, A. Donohoe, A. J. Brady, N. M. Moyna, G. Wallace, D. Diamond and M. McCaul, *Talanta*, 2020, **219**, 121145.

117 H. Veeze, *Neth. J. Med.*, 1995, **46**, 271–274.

118 A. Mishra, R. Greaves, K. Smith, J. B. Carlin, A. Wootton, R. Stirling and J. Massie, *J. Pediatr.*, 2008, **153**, 758–763.e1.

119 A. la Grasta, M. De Carlo, A. Di Nisio, F. Dell'Olio and V. M. N. Passaro, *Sensors*, 2023, **23**, 2491.

120 R. Biswas, *JBMOA*, 2022, **10**, 66–67.

121 T. R. Ray, M. Ivanovic, P. M. Curtis, D. Franklin, K. Guventurk, W. J. Jeang, J. Chafetz, H. Gaertner, G. Young, S. Rebollo, J. B. Model, S. P. Lee, J. Ciraldo, J. T. Reeder, A. Hourlier-Fargette, A. J. Bandodkar, J. Choi, A. J. Aranyosi, R. Ghaffari, S. A. McColley, S. Haymond and J. A. Rogers, *Sci. Transl. Med.*, 2021, **13**, eabd8109.

122 L. B. Baker, *Sports Med.*, 2017, **47**, 111–128.

123 Office of Dietary Supplements - Potassium, <https://ods.od.nih.gov/factsheets/Potassium-HealthProfessional/>, (accessed 24 April 2023).

124 B. Liang, Q. Cao, X. Mao, W. Pan, T. Tu, L. Fang and X. Ye, *IEEE Sens. J.*, 2021, **21**, 9642–9648.

125 J. R. Sempionatto, M. Lin, L. Yin, E. De la Paz, K. Pei, T. Sonsard, A. N. de Loyola Silva, A. A. Khorshed, F. Zhang, N. Tostado, S. Xu and J. Wang, *Nat. Biomed. Eng.*, 2021, **5**, 737–748.

126 J. R. Sempionatto, T. Nakagawa, A. Pavinatto, S. T. Mensah, S. Imani, P. Mercier and J. Wang, *Lab Chip*, 2017, **17**, 1834–1842.

127 J. Xiao, Y. Liu, L. Su, D. Zhao, L. Zhao and X. Zhang, *Anal. Chem.*, 2019, **91**, 14803–14807.

128 G. Xiao, J. He, X. Chen, Y. Qiao, F. Wang, Q. Xia, L. Yu and Z. Lu, *Cellulose*, 2019, **26**, 4553–4562.

129 G. Bolat, E. De La Paz, N. F. Azeredo, M. Kartolo, J. Kim, A. N. De Loyola, E. Silva, R. Rueda, C. Brown, L. Angnes, J. Wang and J. R. Sempionatto, *Anal. Bioanal. Chem.*, 2022, **414**, 5411–5421.

130 Y. Y. Al-Tamer, E. A. Hadi and I. E. I. Al-Badrani, *Urol. Res.*, 1997, **25**, 337–340.

131 X. Wang, S. Chen, X. Tang, D. Lin and P. Qiu, *RSC Adv.*, 2019, **9**, 36578–36585.

132 D. I. Jalal, *Curr. Med. Res. Opin.*, 2016, **32**, 1863–1869.

133 Z. Xu, J. Song, B. Liu, S. Lv, F. Gao, X. Luo and P. Wang, *Sens. Actuators, B*, 2021, **348**, 130674.

134 A. N. Balaji, C. Yuan, B. Wang, L.-S. Peh and H. Shao, in *Proceedings of the 17th Annual International Conference on Mobile Systems, Applications, and Services*, ACM, Seoul Republic of Korea, 2019, pp. 262–274.

135 P. Escobedo, C. E. Ramos-Lorente, A. Martínez-Olmos, M. A. Carvajal, M. Ortega-Muñoz, I. de Orbe-Payá, F. Hernández-Mateo, F. Santoyo-González, L. F. Capitán-Vallvey, A. J. Palma and M. M. Erenas, *Sens. Actuators, B*, 2021, **327**, 128948.

136 H. Y. Y. Nyein, M. Bariya, B. Tran, C. H. Ahn, B. J. Brown, W. Ji, N. Davis and A. Javey, *Nat. Commun.*, 2021, **12**, 1823.

137 Y. Yu, I. Prassas, C. M. J. Muytjens and E. P. Diamandis, *J. Proteomics*, 2017, **155**, 40–48.

138 K. Ngamchuea, K. Chaisiwamongkhol, C. Batchelor-McAuley and R. G. Compton, *Analyst*, 2018, **143**, 81–99.

139 E. Papacosta and G. P. Nassis, *J. Sci. Med. Sport*, 2011, **14**, 424–434.

140 G. Iorgulescu, *J. Med. Life*, 2009, **2**, 303–307.

141 M. Dodds, S. Roland, M. Edgar and M. Thornhill, *BDJ Team*, 2015, **2**, 15123.

142 R. S. P. Malon, S. Sadir, M. Balakrishnan and E. P. Córcoles, *Biomed Res. Int.*, 2014, **2014**, 1–20.

143 O. R. Barley, D. W. Chapman and C. R. Abbiss, *J. Int. Soc. Sports Nutr.*, 2020, **17**, 52.

144 M. Villiger, R. Stoop, T. Vetsch, E. Hohenauer, M. Pini, P. Clarys, F. Pereira and R. Clijsen, *Eur. J. Clin. Nutr.*, 2018, **72**, 69–76.

145 G. Selvolini, A.-M. Drăgan, G. Melinte, C. Cristea and G. Marrazza, in *Sensors and Microsystems*, ed. G. Di Francia and C. Di Natale, Springer International Publishing, Cham, 2023, vol. 918, pp. 3–7.

146 L. F. de Castro, S. V. de Freitas, L. C. Duarte, J. A. C. de Souza, T. R. L. C. Paixão and W. K. T. Coltro, *Anal. Bioanal. Chem.*, 2019, **411**, 4919–4928.

147 M. J. Kangas, R. M. Burks, J. Atwater, R. M. Lukowicz, P. Williams and A. E. Holmes, *Crit. Rev. Anal. Chem.*, 2017, **47**, 138–153.

148 T. Arakawa, K. Tomoto, H. Nitta, K. Toma, S. Takeuchi, T. Sekita, S. Minakuchi and K. Mitsubayashi, *Anal. Chem.*, 2020, **92**, 12201–12207.

149 L. García-Carmona, A. Martín, J. R. Sempionatto, J. R. Moreto, M. C. González, J. Wang and A. Escarpa, *Anal. Chem.*, 2019, **91**, 13883–13891.

150 J. Ballesta Claver, M. C. Valencia Mirón and L. F. Capitán-Vallvey, *Analyst*, 2009, **134**, 1423.

151 K. Suneetha and T. Rambabu, *Indian J. Endocrinol. Metab.*, 2012, **16**, 665.

152 P. Swetha, U. Balijapalli and S.-P. Feng, *Electrochem. Commun.*, 2022, **140**, 107314.

153 A.-M. Spehar-Délèze, S. Anastasova and P. Vadgama, *Chemosensors*, 2021, **9**, 195.

154 J. Kim, G. Valdés-Ramírez, A. J. Bandodkar, W. Jia, A. G. Martínez, J. Ramírez, P. Mercier and J. Wang, *Analyst*, 2014, **139**, 1632–1636.

155 Q. U. Khan, *Cureus*, 2020, **12**(11), e11548.

156 L. F. Hofman, *J. Nutr.*, 2001, **131**, 1621S–1625S.

157 M. A. Laine and A. O. Ojanotko, *J. Steroid Biochem. Mol. Biol.*, 1999, **70**, 109–113.

158 A. Diago-Galmés, C. Guillamón-Escudero, J. M. Tenías-Burillo, J. M. Soriano and J. Fernández-Garrido, *Biology*, 2021, **10**, 93.

159 B. Keevil, P. MacDonald, W. Macdowall, D. Lee, F. Wu and The NATSAL Team, *Ann. Clin. Biochem.*, 2014, **51**, 368–378.

160 M. S. Khan, S. K. Misra, Z. Wang, E. Daza, A. S. Schwartz-Duval, J. M. Kus, D. Pan and D. Pan, *Anal. Chem.*, 2017, **89**, 2107–2115.

161 R. D. Goll and B. K. Mookerjee, *J. Dial.*, 1978, **2**, 399–414.

162 J. Kim, S. Imani, W. R. de Araujo, J. Warchall, G. Valdés-Ramírez, T. R. L. C. Paixão, P. P. Mercier and J. Wang, *Biosens. Bioelectron.*, 2015, **74**, 1061–1068.

163 P. Brandtzaeg, *J. Oral Microbiol.*, 2013, **5**, 20401.

164 M. reviewed by D. C. L. D Pharm, Immunoglobulin Types and Their Functions, <https://ameripharmaspecialty.com/immunoglobulins-ig/>, (accessed 26 April 2023).

165 M. S. Mannoor, H. Tao, J. D. Clayton, A. Sengupta, D. L. Kaplan, R. R. Naik, N. Verma, F. G. Omenetto and M. C. McAlpine, *Nat. Commun.*, 2012, **3**, 763.

166 J. Ceron, E. Lamy, S. Martinez-Subiela, P. Lopez-Jornet, F. Capela-Silva, P. Eckersall and A. Tvarijonaviciute, *JCM*, 2020, **9**, 1491.

167 S. Baliga, S. Muglikar and R. Kale, *J. Indian Soc. Periodontol.*, 2013, **17**, 461.

168 G. Matzeu, G. R. S. Naveh, S. Agarwal, J. A. Roshko, N. A. Ostrovsky-Snider, B. S. Napier and F. G. Omenetto, *Adv. Sci.*, 2021, **8**, 2003416.

169 S. Mondal, S. Karuppuswami, R. Steinhorst and P. Chahal, in *2019 IEEE 69th Electronic Components and Technology Conference (ECTC)*, IEEE, Las Vegas, NV, USA, 2019, pp. 1240–1245.

170 M. Adabi, M. Naghibzadeh, M. Adabi, M. A. Zarrinford, S. S. Esnaashari, A. M. Seifalian, R. Faridi-Majidi, H. Tanimowo Aiyelabegan and H. Ghanbari, *Artif. Cells, Nanomed., Biotechnol.*, 2017, **45**, 833–842.

171 J. Kim, A. S. Campbell, B. E.-F. De Ávila and J. Wang, *Nat. Biotechnol.*, 2019, **37**, 389–406.

172 A. J. Bandodkar, W. Jia, C. Yardımcı, X. Wang, J. Ramirez and J. Wang, *Anal. Chem.*, 2015, **87**, 394–398.

173 H. C. Ates, P. Q. Nguyen, L. Gonzalez-Macia, E. Morales-Narváez, F. Güder, J. J. Collins and C. Dincer, *Nat. Rev. Mater.*, 2022, **7**, 887–907.

174 P. J. Stout, N. Peled, B. J. Erickson, M. E. Hilgers, J. R. Racchini and T. B. Hoegh, *Diabetes Technol. Ther.*, 2001, **3**, 81–90.

175 N. Kashaninejad, A. Munaz, H. Moghadas, S. Yadav, M. Umer and N.-T. Nguyen, *Chemosensors*, 2021, **9**, 83.

176 K. Takeuchi, N. Takama, B. Kim, K. Sharma, O. Paul and P. Rutherford, *Biomed. Microdevices*, 2019, **21**, 28.

177 J. Kim, J. R. Sempionatto, S. Imani, M. C. Hartel, A. Barfodokht, G. Tang, A. S. Campbell, P. P. Mercier and J. Wang, *Adv. Sci.*, 2018, **5**, 1800880.

178 T. Siegmund, L. Heinemann, R. Kolassa and A. Thomas, *J. Diabetes Sci. Technol.*, 2017, **11**, 766–772.

179 A. Facchinetti, G. Sparacino and C. Cobelli, *J. Diabetes Sci. Technol.*, 2007, **1**, 617–623.

180 Z. Pu, X. Zhang, H. Yu, J. Tu, H. Chen, Y. Liu, X. Su, R. Wang, L. Zhang and D. Li, *Sci. Adv.*, 2021, **7**, eabd0199.

181 Join My Freestyle - FreeStyle Libre|Abbott, <https://www.freestyleabbott.in-en/myfreestyle.html>, (accessed 8 April 2023).

182 Dexcom G6 CGM System|No Fingersticks, No Scanning|Dexcom, <https://www.dexcom.com/en-us/g6-cgm-system>, (accessed 8 April 2023).

183 Introducing the Eversense® E3 CGM System|Ascensia Diabetes Care, <https://www.ascensiadiabetes.com/eversense/>, (accessed 8 April 2023).

184 Guardian Connect Continuous Glucose Monitoring|Medtronic, <https://www.medtronicdiabetes.com/products/guardian-connect-continuous-glucose-monitoring-system>, (accessed 8 April 2023).

185 MiniMed Revel Insulin Pump|Medtronic Diabetes, <https://www.medtronicdiabetes.com/customer-support/minimed-revel-insulin-pump>, (accessed 8 April 2023).

186 T. Hutter, T. S. Collings, G. Kostova and F. E. Karet Frankl, *Sens. Diagn.*, 2022, **1**, 614–626.

187 M. Parrilla, M. Cuartero, S. Padrell Sánchez, M. Rajabi, N. Roxhed, F. Niklaus and G. A. Crespo, *Anal. Chem.*, 2019, **91**, 1578–1586.

188 P. R. Miller, X. Xiao, I. Brener, D. B. Burckel, R. Narayan and R. Polksky, *Adv. Healthcare Mater.*, 2014, **3**, 876–881.

189 Á. Molinero-Fernández, A. Casanova, Q. Wang, M. Cuartero and G. A. Crespo, *ACS Sens.*, 2023, **8**, 158–166.

190 J. J. García-Guzmán, C. Pérez-Ràfols, M. Cuartero and G. A. Crespo, *ACS Sens.*, 2021, **6**, 1129–1137.

191 J. J. García-Guzmán, C. Pérez-Ràfols, M. Cuartero and G. A. Crespo, *ACS Sens.*, 2021, **6**, 1129–1137.

192 R. K. Mishra, K. Y. Goud, Z. Li, C. Moonla, M. A. Mohamed, F. Tehrani, H. Teymourian and J. Wang, *J. Am. Chem. Soc.*, 2020, **142**, 5991–5995.

193 K. Y. Goud, C. Moonla, R. K. Mishra, C. Yu, R. Narayan, I. Litvan and J. Wang, *ACS Sens.*, 2019, **4**, 2196–2204.

194 C. Cobelli, M. Schiavon, C. Dalla Man, A. Basu and R. Basu, *Diabetes Technol. Ther.*, 2016, **18**, 505–511.

195 D. Ami, A. Duse, P. Mereghetti, F. Cozza, F. Ambrosio, E. Ponzini, R. Grandori, C. Lunetta, S. Tavazzi, F. Pezzoli and A. Natalello, *Anal. Chem.*, 2021, **93**, 16995–17002.

196 Y. Shi, N. Jiang, P. Bikkannavar, M. F. Cordeiro and A. K. Yetisen, *Analyst*, 2021, **146**, 6416–6444.

197 A. K. Yetisen, N. Jiang, A. Tamayol, G. U. Ruiz-Esparza, Y. S. Zhang, S. Medina-Pando, A. Gupta, J. S. Wolffsohn, H. Butt, A. Khademhosseini and S.-H. Yun, *Lab Chip*, 2017, **17**, 1137–1148.

198 K. Yamada, S. Takaki, N. Komuro, K. Suzuki and D. Citterio, *Analyst*, 2014, **139**, 1637.

199 A. Daily, P. Ravishankar, S. Harms and V. S. Klimberg, *PLoS One*, 2022, **17**, e0267676.

200 M. Elsherif, M. U. Hassan, A. K. Yetisen and H. Butt, *ACS Nano*, 2018, **12**, 5452–5462.

201 H. Teymourian, M. Parrilla, J. R. Sempionatto, N. F. Montiel, A. Barfidokht, R. Van Echelpoel, K. De Wael and J. Wang, *ACS Sens.*, 2020, **5**, 2679–2700.

202 M. Aihara, N. Kubota, T. Minami, R. Shirakawa, Y. Sakurai, T. Hayashi, M. Iwamoto, I. Takamoto, T. Kubota, R. Suzuki, S. Usami, H. Jinnouchi, M. Aihara, T. Yamauchi, T. Sakata and T. Kadokawa, *J. Diabetes Invest.*, 2021, **12**, 266–276.

203 H. Kudo, T. Sawada, E. Kazawa, H. Yoshida, Y. Iwasaki and K. Mitsubayashi, *Biosens. Bioelectron.*, 2006, **22**, 558–562.

204 M. Chu, T. Shirai, D. Takahashi, T. Arakawa, H. Kudo, K. Sano, S. Sawada, K. Yano, Y. Iwasaki, K. Akiyoshi, M. Mochizuki and K. Mitsubayashi, *Biomed. Microdevices*, 2011, **13**, 603–611.

205 X. Yang, H. Yao, G. Zhao, G. A. Ameer, W. Sun, J. Yang and S. Mi, *J. Mater. Sci.*, 2020, **55**, 9551–9561.

206 P. T. Khaw, *BMJ*, 2004, **328**, 97–99.

207 S. Agaoglu, P. Diep, M. Martini, S. Kt, M. Baday and I. E. Araci, *Lab Chip*, 2018, **18**, 3471–3483.

208 J. Bader, M. Zeppieri and S. J. Havens, in *StatPearls [Internet]*, StatPearls Publishing, 2022.

209 A. E. Kownacka, D. Vegelyte, M. Joosse, N. Anton, B. J. Toebe, J. Lauko, I. Buzzacchera, K. Lipinska, D. A. Wilson, N. Geelhoed-Duijvestijn and C. J. Wilson, *Biomacromolecules*, 2018, **19**, 4504–4511.

210 S. R. Corrie, J. W. Coffey, J. Islam, K. A. Markey and M. A. F. Kendall, *Analyst*, 2015, **140**, 4350–4364.

211 M. H. M. Kouhani, J. Wu, A. Tavakoli, A. J. Weber and W. Li, *Lab Chip*, 2020, **20**, 332–342.

212 W. Yang, X. Zhang, Y. Wang, Q. Fan, S. Zhang, Y. Chen, X. Shen, M. Xie and X. Duan, *Appl. Phys. Lett.*, 2021, **119**, 193701.

213 H. An, L. Chen, X. Liu, B. Zhao, H. Zhang and Z. Wu, *Sens. Actuators, A*, 2019, **295**, 177–187.

214 Y. Zhu, R. Nasiri, E. Davoodi, S. Zhang, S. Saha, M. Linn, L. Jiang, R. Haghniaz, M. C. Hartel, V. Jucaud, M. R. Dokmeci, A. Herland, E. Toyserkani and A. Khademhosseini, *Small*, 2023, **19**, 2207017.

215 J. R. Sempionatto, L. C. Brazaca, L. García-Carmona, G. Bolat, A. S. Campbell, A. Martin, G. Tang, R. Shah, R. K. Mishra, J. Kim, V. Zucolotto, A. Escarpa and J. Wang, *Biosens. Bioelectron.*, 2019, **137**, 161–170.

216 J. Xu, X. Tao, X. Liu and L. Yang, *Anal. Chem.*, 2022, **94**, 8659–8667.

217 C.-C. Lin, C.-C. Tseng, T.-K. Chuang, D.-S. Lee and G.-B. Lee, *Analyst*, 2011, **136**, 2669.

218 Z. Zhang, J. Liu, Y. Cheng, J. Chen, H. Zhao and X. Ren, *Front. Anal. Sci.*, 2022, **1**, 812301.

219 D. Martens, P. Ramirez-Priego, M. S. Murib, A. A. Elamin, A. B. Gonzalez-Guerrero, M. Stehr, F. Jonas, B. Anton, N. Hlawatsch, P. Soetaert, R. Vos, A. Stassen, S. Severi, W. Van Roy, R. Bockstaele, H. Becker, M. Singh, L. M. Lechuga and P. Bienstman, *Anal. Methods*, 2018, **10**, 3066–3073.

220 C. Gnoth and S. Johnson, *Geburtshilfe Frauenheilkd.*, 2014, **74**, 661–669.

221 N. K. Griffin, M. A. Smith, P. A. Jenkins, G. Werther and J. D. Baum, *Arch. Dis. Child.*, 1979, **54**, 371–374.

222 H. Blotner, *JAMA*, 1946, **131**, 1109.

223 K. Phoonsawat, T. Ozer, W. Dungchai and C. S. Henry, *Analyst*, 2022, **147**, 4517–4524.

224 Y. Zhou and Z. Cai, *Rapid Commun. Mass Spectrom.*, 2020, **34**(S1), DOI: [10.1002/rcm.8583](https://doi.org/10.1002/rcm.8583).

225 R. A. Leiva, T. P. Bouchard, S. H. Abdullah and R. Ecochard, *Front. Public Health*, 2017, **5**, 320.

226 A. Z. Steiner, D. L. Long, A. H. Herring, J. S. Kesner, J. W. Meadows and D. D. Baird, *Reprod. Sci.*, 2013, **20**, 549–556.

227 A. Plenis, L. Konieczna, I. Olędzka, P. Kowalski and T. Bączek, *Mol. BioSyst.*, 2011, **7**, 1487.

228 O. Olivieri, D. Cecconi, A. Castagna, L. Chiechi, P. Guarini, M. Gunasekaran, F. Morandini, P. Brazzarola, L. Zolla, A. D'Alessandro, F. Veglio, P. Mularo and F. Pizzolo, *Mol. BioSyst.*, 2014, **10**, 1281.

229 J. Ye, N. Li, Y. Lu, J. Cheng and Y. Xu, *Anal. Methods*, 2017, **9**, 2464–2471.

230 T. Liabsuetrakul, S. Srisook, K. Jandee and R. Mori, *Hypertension Research in Pregnancy*, 2021, **9**, 75–81.

231 M. Ra, M. S. Muhammad, C. Lim, S. Han, C. Jung and W.-Y. Kim, *IEEE J. Transl. Eng. Health Med.*, 2018, **6**, 1–11.

232 I. P. Korneeva, K. A. Kramar, T. M. Magrupov and E. A. Semenova, in *2021 International Conference on Information Science and Communications Technologies (ICISCT)*, IEEE, Tashkent, Uzbekistan, 2021, pp. 1–4.

233 G. Liu, N. Hu, Z. Ma and R. Li, *J. Instrum.*, 2018, **13**, T07002.

234 X. Li, C. Zhan, Q. Huang, M. He, C. Yang, C. Yang, X. Huang, M. Chen, X. Xie and H.-J. Chen, *ACS Appl. Nano Mater.*, 2022, **5**, 4767–4778.

235 S. Cho, T. S. Park, T. G. Nahapetian and J.-Y. Yoon, *Biosens. Bioelectron.*, 2015, **74**, 601–611.

236 H. Li, S. Gu, Q. Zhang, E. Song, T. Kuang, F. Chen, X. Yu and L. Chang, *Nanoscale*, 2021, **13**, 3436–3453.

237 F. S. H. Krismastuti, W. L. A. Brooks, M. J. Sweetman, B. S. Sumerlin and N. H. Voelcker, *J. Mater. Chem. B*, 2014, **2**, 3972–3983.

238 S. Barrientos, H. Brem, O. Stojadinovic and M. Tomic-Canic, *Wound Repair Regen*, 2014, **22**, 569–578.

239 E. Rezvani Ghomi, S. Khalili, S. Nouri Khorasani, R. Esmaily Neisiany and S. Ramakrishna, *J. Appl. Polym. Sci.*, 2019, **136**, 47738.

240 S. Dhivya, V. V. Padma and E. Santhini, *BioMed*, 2015, **5**, 22.

241 G. Shabestani Monfared, P. Ertl and M. Rothbauer, *Pharmaceutics*, 2021, **13**, 793.

242 Y.-C. Chuang, V. Tyagi, R.-T. Liu, M. B. Chancellor and P. Tyagi, *Urol. Sci.*, 2010, **21**, 132–136.

243 R.-Y. Xu, H.-W. Liu, J.-L. Liu and J.-H. Dong, *BMC Urol.*, 2014, **14**, 45.

244 P. Mostafalu, A. Tamayol, R. Rahimi, M. Ochoa, A. Khalilpour, G. Kiaee, I. K. Yazdi, S. Bagherifard, M. R. Dokmeci, B. Ziaie, S. R. Sonkusale and A. Khademhosseini, *Small*, 2018, **14**, 1703509.

245 P. Rajput, *et al.*, *TURCOMAT*, 2021, **12**(5), 1650–1662.

246 B. Qiao, Q. Pang, P. Yuan, Y. Luo and L. Ma, *Biomater. Sci.*, 2020, **8**, 1649–1657.

247 J. F. Lo, M. Brennan, Z. Merchant, L. Chen, S. Guo, D. T. Eddington and L. A. DiPietro, *Wound Repair Regen*, 2013, **21**, 226–234.

248 S. Shaner, A. Savelyeva, A. Kvartuh, N. Jedrusik, L. Matter, J. Leal and M. Asplund, *Lab Chip*, 2023, **23**, 1531–1546.

249 Microfluidic spinning-induced heterotypic bead-on-string fibers for dual-cargo release and wound healing - *Journal of Materials Chemistry B* (RSC Publishing), <https://pubs.rsc.org/en/content/articlelanding/2021/tb/d0tb02305a>, (accessed 13 April 2023).

250 W. Zhao, Y. Zhang, L. Liu, Y. Gao, W. Sun, Y. Sun and Q. Ma, *J. Mater. Chem. B*, 2022, **10**, 8357–8374.

251 F. Hu, Q. Gao, J. Liu, W. Chen, C. Zheng, Q. Bai, N. Sun, W. Zhang, Y. Zhang and T. Lu, *J. Mater. Chem. B*, 2023, **11**, 2830–2851.

252 Q. Huang, F. He, J. Yu, J. Zhang, X. Du, Q. Li, G. Wang, Z. Yu and S. Chen, *J. Mater. Chem. B*, 2021, **9**, 2727–2735.

253 M. Ochoa, R. Rahimi, J. Zhou, H. Jiang, C. K. Yoon, D. Maddipatla, B. B. Narakathu, V. Jain, M. M. Osca, T. J. Morken, R. H. Oliveira, G. L. Campana, O. W. Cummings, M. A. Zieger, R. Sood, M. Z. Atashbar and B. Ziaie, *Microsyst. Nanoeng.*, 2020, **6**, 46.

254 H. Levitt, *Trends in Amplification*, 2007, **11**, 7–24.

255 L. Liu, M. Bi, Y. Wang, J. Liu, X. Jiang, Z. Xu and X. Zhang, *Nanoscale*, 2021, **13**, 19352–19366.

256 Wearable Devices and the Internet of Things|Mouser, <https://au.mouser.com/applications/article-iot-wearable-devices/>, (accessed 8 July 2023).

257 Age of AI: Everything you need to know about artificial intelligence|TechCrunch, <https://techcrunch.com/2023/07/07/age-of-ai-everything-you-need-to-know-about-artificial-intelligence/>, (accessed 8 July 2023).

258 J. Srivastava, S. Routray, S. Ahmad and M. M. Waris, *Comput. Intell. Neurosci.*, 2022, **2022**, 1–17.

259 Wearables and AI will be The Game Changer in Healthcare - Digital Salutem, <https://digitalsalutem.com/wearables-and-ai-in-healthcare/>, (accessed 8 July 2023).

260 S. Cheng, Z. Gu, L. Zhou, M. Hao, H. An, K. Song, X. Wu, K. Zhang, Z. Zhao, Y. Dong and Y. Wen, *Front. Bioeng. Biotechnol.*, 2021, **9**, 765987.

261 Artificial Intelligence Market Size, Share, Growth Report 2030, <https://www.grandviewresearch.com/industry-analysis/artificial-intelligence-ai-market>, (accessed 8 July 2023).

262 What is Artificial Intelligence (AI)?, <https://www.ibm.com/topics/artificial-intelligence>, (accessed 8 July 2023).

263 H. Liu, L. Nan, F. Chen, Y. Zhao and Y. Zhao, *Lab Chip*, 2023, **23**, 2497–2513.

264 N. H. Bhuiyan, J. H. Hong, M. J. Uddin and J. S. Shim, *Anal. Chem.*, 2022, **94**, 3872–3880.

265 X. Ma, G. Guo, X. Wu, Q. Wu, F. Liu, H. Zhang, N. Shi and Y. Guan, *Micromachines*, 2023, **14**, 972.

266 W. Lee, A. Gonzalez, P. Arguelles, R. Guevara, M. J. Gonzalez-Guerrero and F. A. Gomez, *Electrophoresis*, 2018, **39**(12), 1443–1451.

267 S. Shajari, K. Kuruvinashetti, A. Komeili and U. Sundararaj, *Sensors*, 2023, **23**, 9498.

268 B. Turan, T. Masuda, W. Lei, A. M. Noor, K. Horio, T. I. Saito, Y. Miyata and F. Arai, *ROBOMECH J.*, 2018, **5**, 27.

269 K. P. Seng, L.-M. Ang, E. Peter and A. Mmonyi, *Electronics*, 2023, **12**, 1509.

270 D. Nahavandi, R. Alizadehsani, A. Khosravi and U. R. Acharya, *Comput. Methods Programs Biomed.*, 2022, **213**, 106541.

271 T. Abe, S. Oh-Hara and Y. Ukita, *Biomicrofluidics*, 2021, **15**, 034101.

272 M. Shayan, S. Bhattacharjee, Y.-A. Song, K. Chakrabarty and R. Karri, *IEEE Trans. Very Large Scale Integr. (VLSI) Syst.*, 2019, **27**, 2755–2766.

273 T. Abe, S. Oh-hara and Y. Ukita, *Biomicrofluidics*, 2022, **16**, 024106.

274 L. B. Baker, M. S. Seib, K. A. Barnes, S. D. Brown, M. A. King, P. J. D. De Chavez, S. Qu, J. Archer, A. S. Wolfe, J. R. Stofan, J. M. Carter, D. E. Wright, J. Wallace, D. S. Yang, S. Liu, J. Anderson, T. Fort, W. Li, J. A. Wright, S. P. Lee, J. B. Model, J. A. Rogers, A. J. Aranyosi and R. Ghaffari, *Adv. Mater. Technol.*, 2022, **7**, 2200249.

275 K. B. Johnson, W. Wei, D. Weeraratne, M. E. Frisse, K. Misulis, K. Rhee, J. Zhao and J. L. Snowdon, *Clin. Transl. Sci.*, 2021, **14**, 86–93.

276 A. Lashkaripour, C. Rodriguez, N. Mehdipour, R. Mardian, D. McIntyre, L. Ortiz, J. Campbell and D. Densmore, *Nat. Commun.*, 2021, **12**, 25.

277 E. A. Galan, H. Zhao, X. Wang, Q. Dai, W. T. S. Huck and S. Ma, *Matter*, 2020, **3**, 1893–1922.

278 M. S. Mahdavinejad, M. Rezvan, M. Barekatain, P. Adibi, P. Barnaghi and A. P. Sheth, *Digit Commun. Netw.*, 2018, **4**, 161–175.

279 Supervised vs. Unsupervised Learning: What's the Difference? | IBM, <https://www.ibm.com/cloud/blog/supervised-vs-unsupervised-learning>, (accessed 8 July 2023).

280 What is Supervised Learning? | IBM, <https://www.ibm.com/topics/supervised-learning>, (accessed 8 July 2023).

281 Supervised and Unsupervised Learning in (Machine Learning), <https://www.simplilearn.com/tutorials/machine-learning-tutorial/supervised-and-unsupervised-learning>, (accessed 8 July 2023).

282 Supervised vs. Unsupervised Learning [Differences & Examples], <https://www.v7labs.com/blog/supervised-vs-unsupervised-learning>, (accessed 8 July 2023).

283 Z. Ao, H. Cai, Z. Wu, L. Hu, A. Nunez, Z. Zhou, H. Liu, M. Bondesson, X. Lu, X. Lu, M. Dao and F. Guo, *Proc. Natl. Acad. Sci. U. S. A.*, 2022, **119**, e2214569119.

284 S. Han, T. Kim, D. Kim, Y.-L. Park and S. Jo, *IEEE Robot. Autom. Lett.*, 2018, **3**, 873–880.

285 V. Rizzuto, A. Mencattini, B. Álvarez-González, D. Di Giuseppe, E. Martinelli, D. Beneitez-Pastor, M. D. M. Mañú-Pereira, M. J. Lopez-Martinez and J. Samitier, *Sci. Rep.*, 2021, **11**, 13553.

286 L. Alzubaidi, J. Zhang, A. J. Humaidi, A. Al-Dujaili, Y. Duan, O. Al-Shamma, J. Santamaría, M. A. Fadhel, M. Al-Amidie and L. Farhan, *J. Big Data*, 2021, **8**, 53.

287 D. McIntyre, A. Lashkaripour, P. Fordyce and D. Densmore, *Lab Chip*, 2022, **22**, 2925–2937.

288 Y. Song, J. Zhao, T. Cai, A. Stephens, S.-H. Su, E. Sandford, C. Flora, B. H. Singer, M. Ghosh, S. W. Choi, M. Tewari and K. Kurabayashi, *Biosens. Bioelectron.*, 2021, **180**, 113088.

289 C. Honrado, J. S. McGrath, R. Reale, P. Bisegna, N. S. Swami and F. Caselli, *Anal. Bioanal. Chem.*, 2020, **412**, 3835–3845.

290 S. Hussein, P. Kandel, C. W. Bolan, M. B. Wallace and U. Bagci, *IEEE Trans. Med. Imaging*, 2019, **38**, 1777–1787.

291 M. Alloghani, D. Al-Jumeily, J. Mustafina, A. Hussain and A. J. Aljaaf, in *Supervised and Unsupervised Learning for Data Science*, ed. M. W. Berry, A. Mohamed and B. W. Yap, Springer International Publishing, Cham, 2020, pp. 3–21.

292 L. B. Baker, M. S. Seib, K. A. Barnes, S. D. Brown, M. A. King, P. J. D. De Chavez, S. Qu, J. Archer, A. S. Wolfe, J. R. Stofan, J. M. Carter, D. E. Wright, J. Wallace, D. S. Yang, S. Liu, J. Anderson, T. Fort, W. Li, J. A. Wright, S. P. Lee, J. B. Model, J. A. Rogers, A. J. Aranyosi and R. Ghaffari, *Adv. Mater. Technol.*, 2022, **7**, 2200249.

293 Q. Ning, W. Zheng, H. Xu, A. Zhu, T. Li, Y. Cheng, S. Feng, L. Wang, D. Cui and K. Wang, *Anal. Bioanal. Chem.*, 2022, **414**, 3959–3970.

294 J. Redmon, S. Divvala, R. Girshick and A. Farhadi, You Only Look Once: Unified, Real-Time Object Detection, *2016 IEEE Conference on Computer Vision and Pattern Recognition (CVPR)*, Las Vegas, NV, USA, 2016, pp. 779–788, DOI: [10.1109/CVPR.2016.91](https://doi.org/10.1109/CVPR.2016.91).

295 P. Mostafalu, M. Akbari, K. A. Alberti, Q. Xu, A. Khademhosseini and S. R. Sonkusale, *Microsyst. Nanoeng.*, 2016, **2**, 16039.

296 A. Sui, W. Sui, S. Liu and R. Rhodes, *Digit. Health*, 2023, **9**, 205520762311537.

297 Y. Li, P. Ni and V. Chang, Ethical problems of smart wearable devices, *COMPLEXIS 2019 - Proceedings of the 4th International Conference on Complexity, Future Information Systems and Risk*, SciTePress, 2019, pp. 121–129, DOI: [10.5220/0007722000520058](https://doi.org/10.5220/0007722000520058).

298 S. Kumar, P. Tiwari and M. Zymbler, *J. Big Data*, 2019, **6**, 111.

299 S. Nižetić, P. Šolić, D. López-de-Ipiña González-de-Artaza and L. Patrono, *J. Cleaner Prod.*, 2020, **274**, 122877.

300 C. Perera, R. Ranjan, L. Wang, S. U. Khan and A. Y. Zomaya, Big Data Privacy in the Internet of Things Era, in *IT Professional*, 2015, vol. 17(3), pp. 32–39, DOI: [10.1109/MITP.2015.34](https://doi.org/10.1109/MITP.2015.34).

301 A. A. Dos-Reis-Delgado, A. Carmona-Dominguez, G. Sosa-Avalos, I. H. Jimenez-Saaib, K. E. Villegas-Cantu, R. C. Gallo-Villanueva and V. H. Perez-Gonzalez, *Electrophoresis*, 2023, **44**, 268–297.

302 A. Haleem, M. Javaid, R. P. Singh and R. Suman, *Sens. Int.*, 2021, **2**, 100117.

303 N. Al Bassam, S. A. Hussain, A. Al Qaraghuli, J. Khan, E. P. Sumesh and V. Lavanya, *Inf. Med. Unlocked*, 2021, **24**, 100588.

304 T. Poongodi, R. Krishnamurthi, R. Indrakumari, P. Suresh and B. Balusamy, in *A Handbook of Internet of Things in Biomedical and Cyber Physical System*, ed. V. E. Balas, V. K. Solanki, R. Kumar and Md. A. R. Ahad, Springer International Publishing, Cham, 2020, vol. 165, pp. 245–273.

305 M. Ibrahim, M. Gorlatova and K. Chakrabarty, in *2019 IEEE/ACM International Conference on Computer-Aided Design (ICCAD)*, IEEE, Westminster, CO, USA, 2019, pp. 1–8.

306 S. M. A. Iqbal, I. Mahgoub, E. Du, M. A. Leavitt and W. Asghar, *npj Flex. Electron.*, 2021, **5**, 9.

307 S. Ardalan, M. Hosseiniard, M. Vosough and H. Golmohammadi, *Biosens. Bioelectron.*, 2020, **168**, 112450.

308 Y. Yuan, S. Feng, M. Alahi, A. Nag, N. Afsarimanesh, H. Zhang and S. He, *Appl. Sci.*, 2018, **8**, 1357.

309 R. Dwivedi, D. Mehrotra and S. Chandra, *J. Oral Biol. Craniofac. Res.*, 2022, **12**, 302–318.

310 M. Conti and A. Passarella, *Comput. Commun.*, 2018, **131**, 51–65.

311 M. Conti, A. Passarella and S. K. Das, *Pervasive Mob. Comput.*, 2017, **41**, 1–27.

312 F. Liu, J.-L. Han, J. Qi, Y. Zhang, J.-L. Yu, W.-P. Li, D. Lin, L.-X. Chen and B.-W. Li, *Chin. J. Anal. Chem.*, 2021, **49**, 159–171.

313 B. Murdoch, *BMC Med. Ethics*, 2021, **22**, 122.

314 P. Esmailzadeh, *BMC Med. Inform. Decis. Mak.*, 2020, **20**, 170.